# Toll links metabolism and microbiota in the *Drosophila* intestine




**A thesis submitted for the degree of Master of Science (by research) in the University of Oxford, Trinity Term 2019**

**Shivohum Bahuguna**

**Hertford College**

**Department of Biochemistry**

# Abstract

Peptidoglycan recognition protein SA (PGRP-SA) is an extracellular recognition protein, which interacts with the peptidoglycan of Gram-positive bacteria and activates the Toll signalling pathway. While many studies have described the interaction of PGRP-SA with pathogenic bacteria, studies on its response to commensal bacteria is lacking. Using *Drosophila melanogaster* as a model organism, we demonstrate the relationship between PGRP-SA with the indigenous gut microbiota, and how the activity of mTOR influences this relationship. Our results reveal that PGRP-SA is essential to maintain microbial load and retain Lactobacillaceae in young flies. Moreover, inhibition of the activity of mTOR restores the microbiota of PGRP-SA mutant *seml* flies in a density dependent manner. Translational regulation factor, 4E-BP, whose levels are dictated by both Toll and mTOR pathway of the host, mediates this host-microbiome interaction. Our results give an insight into how host factors maintain indigenous microbiota in a healthy gut. This can help us better understand the genetic basis of variation in the composition of gut bacteria, and assist in developing measures to tackle microbiota induced disorders in the future.

# Acknowledgement

I would first like to thank my supervisor, Prof. Petros Ligoxygakis for taking me as an MSc by research student and believing in me with such an important project. He has always guided me, motivated me, and encouraged me to frame experiments and solve problems. He always confidently stood by me when my experiments failed in the beginning and taught me that failure is the biggest learning experience for a student. I am truly honoured to have him as a supervising professor and hope the best for his lab.

I am really thankful to all the wonderful members of the lab: Dr Megan Sloan, who has never let any of my questions go unanswered, and has played a major role in correcting and teaching me how to write a thesis. She is a brilliant senior to have, and will truly make a great scientist in the future. I would like to thank Srishti Arora, who has been a great lab member and at the same time, an amazing friend. I am grateful to Dr Ilias Kounatidis, who took out time from his busy schedule at the Diamond light source, to teach me 16S data analysis, and for guiding me and correcting my thesis. A special mention to my first undergrad trainee Dohun Lee, who enthusiastically performed experiments with me and helped me in obtaining important data for the project. I would also like to thank other members of the lab for assisting me in day to day lab activities, and providing moral and technical support. I would like to thank Dr Naomi Patela, who taught me how to make DNA libraries for sequencing, and Dr Richard Parton, who trained me in imaging

and supported my research throughout the year.

I would also like to thank Antony Knight and Anthony Bywaters (Media kitchen), Prof Mark Howarth (Thesis committee), Prof Andre Furger (Thesis committee), and Prof Stephan Uphoff (Department advisor) for their support throughout my degree. I would like to share my sincere thanks to Prof Lynne Cox for taking out time to correct my thesis, and Prof Stuart Ferguson for giving me inputs on my project.

I am very thankful to my close friends (Natasha Jeppu, Adita Agarwal, Shree Sowndarya, Mayur Saxena, Varnika Agarwal, Viveka Kulharia, Aditi Agrawal and Hemani Chhabra), who have made my time at Oxford a truly unforgettable one. I would also like to thank Anurag Srivastava, who has been my mentor, guided me since my undergraduate degree and kept me motivated at difficult times.

Lastly and most importantly, I would like to thank my parents, Deepak and Priya Bahuguna for their support throughout my student life. They have taught me how to take correct decisions and be optimistic. Without their help and support, I would not have been able to become the person I am today.

-Shivohum Bahuguna, September 2019

# Contents

**Abstract** . . . . . **i**

**Acknowledgement** . . . . . **ii**

**List of Figures** . . . . . **viii**

**List of Tables** . . . . . **xii**

**Abbreviations** . . . . . **xiii**

**1 Introduction** . . . . . **1**

1.1 Microbial composition of the gut in humans and animal models 1

1.1.1 Composition of commensal microbiota in human gut . 2

1.1.2 Composition of *Drosophila melanogaster* gut microbiome 4

1.2 Host microbial interaction in *Drosophila* gut . . . . . 8

1.2.1 Relationship between host immunity and gut microbiota 8

1.2.2 Relationship between diet, metabolism and gut microbiota . . . . . 13

1.2.3 Interaction between immunity and metabolism . . . . . 22

1.3 Aims of the study . . . . . 23

**2 Materials and Methods** . . . . . **25**

2.1 *Drosophila* stocks, and genetics . . . . . 25

2.2 *Drosophila* husbandry . . . . . 25

2.3 Characterization of the *Drosophila* gut microbiota . . . . . 27
2.3.1 Culture dependent quantification of gut microbiota . . 27
2.3.2 Culture independent identification of gut microbiota . . 28
2.4 Lifespan analysis . . . . . 35
2.5 Measuring gene expression in *Drosophila* . . . . . 36
2.5.1 RNA isolation . . . . . 36
2.5.2 cDNA preparation . . . . . 36
2.5.3 Quantitative PCR . . . . . 37
2.5.4 Analysis of qPCR data . . . . . 37

**3 Results . . . . . 39**
3.1 Loss of PGRP-SA changes cultivable microbial density in young flies . . . . . 39
3.2 PGRP-SA associated protein GNBP1 also influences cultivable microbial density in flies . . . . . 43
3.3 The NF-$\kappa$B homologue DIF influences cultivable bacteria in the *Drosophila* gut . . . . . 44
3.4 Young PGRP-SA mutant flies lack Lactobacillaceae . . . . . 46
3.5 Rapamycin does not effect the microbial diversity of young *seml* mutant flies . . . . . 52
3.6 Loss of mTOR activity in the gut restores cultivable microbiota in *seml* flies . . . . . 65

3.7 Loss of PGRP-SA and DIF alters 4E-BP mRNA levels in young flies . . . . . 67
3.8 Restoration is associated with 4E-BP mRNA levels . . . . . 69
3.9 Toll associated NF-$\kappa$B DIF mutants have a reduced lifespan. . 73

**4 Discussion . . . . . 75**
4.1 The *Drosophila* Toll signalling pathway interacts with the intestinal microbiota via the peptidoglycan recognition protein PGRP-SA . . . . . 75
4.2 PGRP-SA promotes Lactobacillaceae retention in young *Drosophila* gut . . . . . 78
4.3 mTOR pathway regulates microbial composition in normal and immune compromised flies . . . . . 78
4.4 Drosophila 4E-BP mediates cross-talk between host-metabolism and immunity with gut microbiota . . . . . 80
4.5 Conclusion . . . . . 81
4.6 Future directions . . . . . 84

**5 Appendix . . . . . 88**
5.1 Appendix 1 . . . . . 88
5.2 Appendix 2 . . . . . 89
5.3 Appendix 3 . . . . . 90
5.4 Appendix 4 . . . . . 91
5.5 Appendix 5 . . . . . 92

5.6 Appendix 6 . . . . . 93
5.7 Appendix 7 . . . . . 94
5.8 Appendix 8 . . . . . 95
5.9 Appendix 9 . . . . . 96

**References** . . . . . **97**

# List of Figures

**1 Introduction** . . . . . **1**

1.1 Gut microbiota composition of *Drosophila melanogaster* . . . . 6

1.2 Gut microbial composition of different model organisms . . . . 7

1.3 The Toll signalling pathway in *Drosophila* . . . . . 10

1.4 mTOR pathway in *Drosophila* . . . . . 19

**2 Materials and Methods** . . . . . **25**

2.1 Wolbachia 16S DNA digestion assay . . . . . 30

2.2 Principle of ion torrent sequencing . . . . . 33

**3 Results** . . . . . **39**

3.1 PGRP-SA influences cultivable microbial load in young *Drosophila* gut. . . . . 40

3.2 Loss of cultivable microbial load is independent of their genetic background in *seml* mutant flies. . . . . 41

3.3 PGRP-SA produced in the enterocyte cells of the gut influences cultivable microbial load in young *Drosophila* . . . . . 42

3.4 Gram-negative bacteria binding protein 1 (GNBP1) influences cultivable microbial load in guts of 5 and 30 day old *Drosophila* 44

3.5 DIF influences cultivable microbial load in young *Drosophila* gut . . . . . 45

3.6 Loss of cultivable microbial load is independent of the genetic background in *dif*[1] mutant flies. . . . . 46
3.7 Effect of loss of PGRP-SA in the gut microbial composition of 5 and 30 day old flies. . . . . 48
3.8 Alpha diversity analysis of *yw* and *yw seml* flies of different ages (5 and 30 day). . . . . 50
3.9 Principal component analysis (PCA) of *yw* and *yw seml* flies of different ages (5 and 30 day). . . . . 51
3.10 Effect of Rapamycin treatment and gut specific knockdown of mTOR on the microbial composition of 5 day old flies. . . . . 55
3.11 Alpha diversity analysis of 5 and 30 day old flies treated with rapamycin and/or carrying $mTOR^{RNAi}$. . . . . 57
3.12 Principal component analysis (PCA) of 5 day old flies treated with rapamycin and/or carrying $mTOR^{RNAi}$. . . . . 58
3.13 Effect of Rapamycin treatment and gut specific knockdown of mTOR on the microbial composition of 30 day old flies. . . . . 61
3.14 Principal component analysis (PCA) of 30 day old flies treated with rapamycin and/or carrying $mTOR^{RNAi}$. . . . . 63
3.15 Principal component analysis (PCA) of 5 and 30 day old *yw* and *yw seml* flies treated with rapamycin and/or carrying $mTOR^{RNAi}$. . . . . 64
3.16 mTOR in the gut is involved in restoration of the cultivable gut microbial load in young *seml* flies. . . . . 65

3.17 Rapamycin restores the cultivable microbial load in *seml* flies . 67
3.18 PGRP-SA and DIF influences 4EBP levels in the *Drosophila* gut. . . . . 68
3.19 Inhibition of mTOR activity restores 4EBP levels in young *seml* mutant *Drosophila* gut. . . . . 70
3.20 4E-BP mediates rapamycin induced restoration of cultivable microbial load in *yw seml* flies. . . . . 72
3.21 Loss of DIF in *yw dif*$^{1}$ mutant flies reduces its lifespan . . . . 73

**4 Discussion . . . . . 75**
4.1 Innate immune Toll signalling pathway and metabolic mTOR pathway interact to shape the gut microbiota of *Drosophila melanogaster* . . . . . 83

**5 Appendix . . . . . 88**
5.1 Relative bacterial abundance of biological repeats of 5 day old *yw* and *yw seml* flies . . . . . 90
5.2 Relative bacterial abundance of enterocyte specific mTOR knock-down flies of different ages. . . . . 91
5.3 Relative bacterial abundance of 5 day old metabolic mutants. 92
5.4 Relative bacterial abundance of 30 day old metabolic mutants. 93
5.5 Components of the mTOR pathway (mTOR, AMPK, and 4E-BP) in the gut influences the cultivable microbial load in young flies. . . . . 95

5.6 Microbial load of *Drosophila melanogaster* depends on the genetic background (*yw* v/s DGRP *25174*). . . . . 96

# List of Tables

**2 Materials and Methods . . . . . 25**

2.1 *Drosophila melanogaster* strains used in this study. . . . . 26

2.2 PCR cycling conditions used to amplify hypervariable regions 1-3 (V1-V3) . . . . . 31

2.3 PCR cycling conditions used to amplify hypervariable region 3 (V3) . . . . . 31

2.4 Primers used for 16S library preparation . . . . . 32

2.5 Primers used to quantify 4E-BP and Rp49 . . . . . 37

**5 Appendix . . . . . 88**

5.1 Fly food composition . . . . . 88

5.2 De Man, Rogosa and Sharpe (MRS) media composition . . . . 89

5.3 $S_{obs}$, Simpson (1-D) and Shannon H alpha diversity index values of different fly lines . . . . . 94

# Abbreviations

| | |
|---|---|
| 4E-BP | Eukaryotic translation initiation factor 4E (eIF4E)-binding protein |
| AMP | Antimicrobial peptides |
| AMPK | Adenosine monophosphate - activated protein kinase |
| ATGL | Adipose triglyceride lipase |
| ATP | Adenosine triphosphate |
| BMI | Body mass index |
| cDNA | Complementary DNA |
| CFU | Colony-forming unit |
| CMOS | Complementary Metal-Oxide Semiconductor |
| Ct | Cycle threshold |
| CyO | Curly O |
| DAP | Diaminopimelic acid |
| DD | Death domain |
| Deptor | DEP domain containing mTOR interacting protein |
| DGRP | Drosophila Genetic Reference Panel |
| Dif | Dorsal-related immunity factor |
| DNA | Deoxyribonucleic acid |
| dNTP | Deoxynucleoside triphosphate |

| | |
|---|---|
| dTOR | Drosophila target of rapamycin |
| Fab | Fragment antigen-binding |
| FOXO | Forkhead box protein O |
| G6PD | Glucose 6-phosphate dehydrogenase |
| gDNA | Genomic DNA |
| GNBP1 | Gram-negative bacteria binding protein 1 |
| GNBP3 | Gram-negative bacteria binding protein 3 |
| Grass | Gram-positive–specific serine protease |
| HSL | Hormone-sensitive lipase |
| IBD | Inflammatory bowel disease |
| IgA | Immunoglobulin A |
| IIS | Insulin/insulin-like growth factor signalling |
| IMD | Immune deficiency pathway |
| ISFET | Ion sensitive field effect transistor |
| *key* | *kenny* |
| LBE | mLST8-binding element |
| Lys | Lysine-type peptidoglycan |
| mLST8 | Mammalian lethal with Sec13 protein 8 |
| ModSP | Modular serine protease |

| | |
|---|---|
| mRNA | Messenger RNA |
| MRS | De Man, Rogosa and Sharpe media |
| mTOR | Mechanistic target of Rapamycin |
| mTORC1/2 | mTOR complex 1/2 |
| NADPH | Nicotinamide adenine dinucleotide phosphate |
| PBS | Phosphate-buffered saline |
| PCA | Principle component analysis |
| PCR | Polymerase chain reaction |
| PFK | Phosphofructokinase |
| PGN | Peptidoglycan |
| PGRP | Peptidoglycan recognition protein |
| PI3K | Phosphoinositide 3-kinases |
| PIKK | Phosphatidylinositol 3-kinase-related kinases |
| PIMS | PGRP-LC-interacting inhibitor of Imd signalling |
| PIP2 | Phosphatidylinositol 4,5 bisphosphate |
| PIP3 | Phosphatidylinositol (3,4,5)-trisphosphate |
| PRAS-40 | Proline-rich Akt substrate of 40 kDa |
| qPCR | Quantitative PCR |
| Rap | Rapamycin |

| | |
|---|---|
| Raptor | Regulatory-associated protein of mTOR |
| REDD1 | Regulated in DNA damage and Development 1 |
| Rictor | Rapamycin insensitive companion of mTOR |
| RNAi | RNA interference |
| RP49 | Ribosomal protein 49 |
| rRNA | Ribosomal RNA |
| S6K1 | p70S6 Kinase 1 |
| SBM | Soybean meal |
| SCFA | Short chain fatty acids |
| *seml* | *semmelweis* |
| SPE | Spz-processing enzyme |
| Spz | Spatzle |
| SREBP | Sterol Regulatory Element Binding Protein |
| TOS | TOR signalling motifs |
| *trbd* | *trabid* |
| TSC1/2 | Tuberous sclerosis 1/2 |
| UAS | Upstream activating sequence |
| *yw* | yellow-white |

# 1 Introduction

## 1.1 Microbial composition of the gut in humans and animal models

Nutrient assimilation is critical for the survival of any organism. The gastrointestinal tract (gut), in association with a highly diverse community of commensal microbes, carries out this function in animals [1].

The mammalian gut has evolved a diverse microbial flora, which assists in regulation of digestion, as well as performing various other roles such as immune development and host signalling [2]. With a count exceeding the total number of human cells by up to 10 times, these microbes colonize various regions of the mammalian body, with most residing in the gut [3]. The host is dependent on these beneficial microbes to provide assistance in its metabolic processes, to supply nutrients/factors, and to resist establishment of pathogens. In order to reap benefits from these microbes, the host provides a symbiotic environment for sustaining them in the gut [4–6].

Disruption of this intimate symbiotic relationship through changes in microbial composition (dysbiosis) has been shown to result in various immune and metabolic disorders, including inflammatory bowel disease (IBD) [7], colorectal cancer [8, 9], obesity [10, 11] and diabetes [12]. Patients with chronic inflammation as a result of IBD have reduced levels of anti-inflammatory

metabolites due to microbial dysbiosis. For example, reduction in levels of butyrate-producing *Faecalibacterium prausnitzii* has been shown in IBD patients [7, 13], as well as in patients with type 2 diabetes [12, 14]. Probiotic treatment, fecal transplantation, and antibiotic treatment can alleviate these disorders by reconstituting a healthy microbial composition [15, 16].

Over the years, multiple theories have been proposed to explain the underlying cause of dysbiosis out of which, the prevailing theory is disruption of immune and/or metabolic pathways [17, 18]. It is therefore important to understand, how host metabolism and immunity are linked, and how together they shape the gut microbiome.

### 1.1.1 Composition of commensal microbiota in human gut

The human body is known to collectively harbour a vast number of microbes belonging to around 500-1000 species, the majority of which reside in the gut [19, 20]. Ninety percent of species in the gut belong to two phyla - Firmicutes and Bacteroidetes, while the rest includes species from Proteobacteria, Verrucomicrobia, Actinobacteria and Fusobacteria [21].

Development of this complex microbial community begins from birth and is acquired through several sources including: maternal transmission during delivery, breastfeeding, diet, and exposure to different environments [22]. Development of the microbiota occurs until three years of age, at which point the microbial composition resembles that of adults [21]. After the age of 70,

there is a decline in microbial diversity, with a decrease in *Bifidobacterium*, and an increase in *Proteobacteria* and *Clostridium*. These changes are attributed to the weakening of the immune system, digestion, and nutrient absorption [21].

Differences in the microbial composition are also observed amongst individuals from different geographical locations, for example in children of rural Africa versus Europe [23]. This difference in the microbial composition was mainly attributed to their disparate diets: African children had a high fibre, low protein diet, whereas European children had a high protein, low fibre diet [23]. Variation in microbial composition amongst individuals of the same population has also been observed in several studies [24, 25]. These variations have been attributed to body mass index (BMI), ethnicity, exercise, diet, and lifestyle [23].

Identifying the underlying causes of microbial variation in humans is challenging due to the inability to directly isolate intestinal microbiota, the complexity of microbial composition, and ethical challenges associated in working with human subjects. To overcome these challenges, model organisms can be used to replicate and study human host-microbe interactions [26].

The fruit fly, *Drosophila melanogaster* is commonly used as a model for studying host-microbial interactions. It is a useful model organism, as it has a less diverse and an easily manipulative gut microbiome compared to humans.

Flies are also cost effective for lab based studies, are easy to rear, and have short generation times/lifespans. Importantly, *Drosophila* and humans share many biological and physiological gut properties [27].

### 1.1.2 Composition of *Drosophila melanogaster* gut microbiome

The *Drosophila* microbiome has a much lower species diversity compared to humans, although Firmicutes dominate the gut microbiome in both humans and fruit flies. Proteobacteria and Firmicutes constitute more than 97% of the *Drosophila* gut microbiome, with Acetobacteraceae and Lactobacillaceae families forming the dominant families [28] **(Figure 1.1)**.

The indigenous gut microbiota of *Drosophila melanogaster* is dynamic, and constantly changes with age and environmental conditions. Bacterial identification studies of the *Drosophila* gut microbiome conducted by Wong *et al.,* (2011) showed a variation in the relative abundance of the five major phyla (Firmicutes, Proteobacteria, Actinobacteria, Bacteroidetes, and Cyanobacteria) in the *Drosophila* gut microbiome, at different stages of life [28]. Sixty-six percent of the microbes on the outer chorion of eggs belonged to the phyla Firmicutes and Proteobacteria. These bacteria constitute the first bacterial community of the fly, and are acquired by larvae when they ingest the chorion [28]. Post ingestion, the microbial load of the larval gut increases until the third instar stage [29]. From the 3rd instar to the adult stage, five species of *Lactobacillus* and *Acetobacter* dominate the gut microbiota [28].

Initially the gut microbiota of a young adult has a low microbial density, due to losses incurred during pupation, and is dominated by *Lactobacillus*. With time, the bacterial load increases and the microbial community shifts towards a dominant *Acetobacter* species together with a reduction in *Lactobacillus* [28]. Similar to humans, these age-related variations are attributed to changes in diet, host metabolism, immunity, and environmental conditions with aging [28, 30].

As observed in humans, inter/intra-population variations have been reported in the gut microbial composition of fruit flies. Inter-population variation was shown by Chandler *et al.,* (2011), who analyzed the microbiome of wild flies caught from different geographical locations (North America to Australia), feeding on different substrates (fruits, flowers, cacti, and mushrooms), and compared them with lab-reared flies [32]. He observed that each of the wild flies showed a different microbial diversity profile, whilst *Acetobacter* and *Lactobacillus* dominated the gut in lab raised flies [32]. Additionally, abundance of Enterobacteriaceae and several pathogenic species of *Erwinia*, *Pantoea*, Providencia, and *Serratia* were found in the guts of wild flies [33]. These differences in the microbial composition were a consequence of difference in diets between wild and lab reared flies [32]. Intra-population variation of the fly gut microbiome has also been observed in isogenic flies reared in different media [32], and in isogenic flies with mutations of immune pathway genes [34]. Similar to the findings in human microbiome studies,

| bacterial genera | Cox & Gilmore 1997 | Ren et al 2007 | Corby et al 2007 | Ryu et al 2008 | Chandler et al 2011 | Wong et al 2011 |
|---|---|---|---|---|---|---|
| *Acetobacter* | +w, l | +l | +w | +l | +w, l | +l |
| *Acidovorax* | | | +w | | | |
| *Acinetobacter* | | | +w | | | |
| *Agrobacterium* | | | +w | | | |
| *Alcaligenes* | | | +w | | | |
| *Arcobacter* | | | +w | | | |
| *Azospirillum* | | | | | | |
| *Bacillus* | +? | | | | | |
| *Bordetella* | | | +w | | | |
| *Bradyrhizobium* | +? | | | | | |
| *Chitinophaga* | +? | | | | | |
| *Citrobacter* | +? | | | | | |
| *Cladosporium* | | +l | | | | |
| *Commensalibacter* | | | | | +w, l | |
| *Corynebacterium* | +w | | | | | |
| *Dysgonomonas* | | | | | +w, l | |
| *Enterobacter* | +? | | +w | | +w, l | |
| *Enterococcus* | +w, l | | +w | | +w | |
| *Erwinia* | +? | | | | +w | |
| *Frateuria* | | | +w | | | |
| *Gluconacetobacter* | | | +w | +l | | |
| *Gluconobacter* | +? | | +w | | | |
| *Klebsiella* | +? | | | | | |
| *Lactobacillus* | +? | +l | +w | +l | +w, l | +l |
| *Leuconostoc* | +? | | +w | | | |
| *Morganella* | +? | | | | | |
| *Pantoea* | +? | | | | + w | |
| *Providencia* | | | +w | | +w, l | |
| *Pseudomonas* | +? | | +w | | | |
| *Serratia* | +? | | | | +w, l | |
| *Shigella* | | | | | +w, l | |
| *Spiroplasma* | | | | | +w | |
| *Staphylococcus* | +? | +l | | | +w | +l |
| *Stenotrophomonas* | +? | | +w | | | |
| *Vagococcus* | | | | | | |
| *Weissella* | +? | | | | | |
| *Wolbachia* | +w | | +w | +l | +w | |

+, present in; l, laboratory strain; w, caught in the wild; ?, not specified; refs. [20,21] gut only, all other whole flies.

**Figure 1.1:** Gut microbiota composition of *Drosophila melanogaster* as observed in six different studies.(+, present in: l-laboratory strain, w-wild caught, ?-not specified). Table adapted from Kounatidis *et al.*, (2012) [31].

variations in the fly gut microbiome have also been linked to immune status, metabolism, and environmental conditions [34–37].

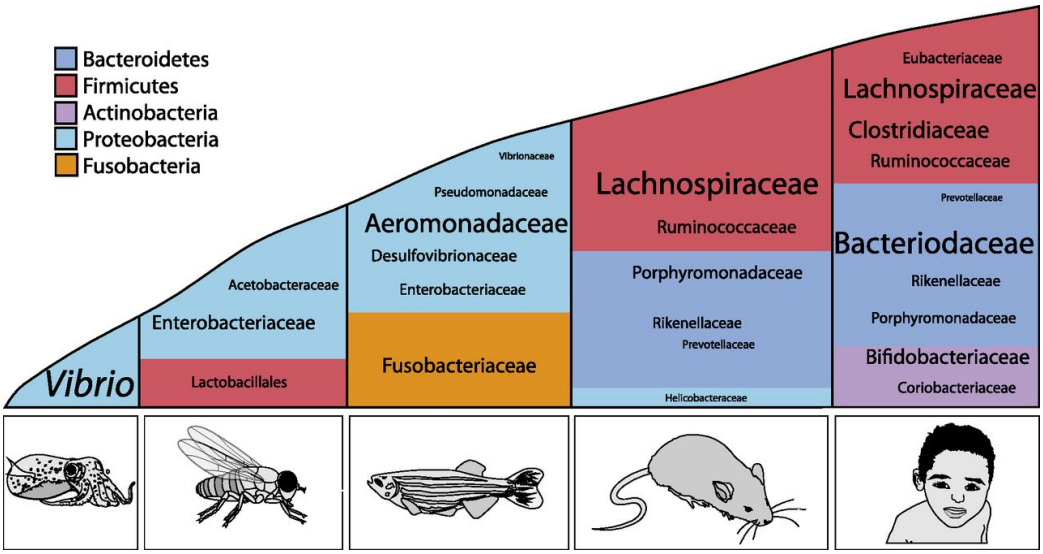



**Figure 1.2:** Illustration of the gut microbial composition of different organisms: *Drosophila*, zebra fish, mouse and humans. Figure adapted from Kostic *et al.,* (2013) [38]

Since Drosophila is commonly used as a model organism to study host microbiome interactions, I chose it to study the role of metabolism and immunity in shaping the gut microbiota of healthy individuals. An understanding of this relationship in flies can give an insight into the human-microbiome system and help to elucidate the cause of dysbiosis in disease.

## 1.2 Host microbial interaction in *Drosophila* gut

### 1.2.1 Relationship between host immunity and gut microbiota

As discussed above, the *Drosophila* gut hosts a wide range of microbial species, which includes both commensal and pathogenic microbes [39]. The *Drosophila* gut has developed various mechanisms to preserve commensal microbes and kill pathogens [40]. In order to eliminate pathogenic bacteria, the gut epithelium initiates innate immune responses via two main pathways: Toll and IMD. These pathways mediate the production of antimicrobial peptides (AMPs) [41]. The IMD pathway has been extensively reviewed elsewhere [42]. This project addresses the role of the Toll signalling pathway which is outlined below:

**Toll signalling pathway**

The Toll signalling pathway **(Figure 1.3)** is an innate immune pathway in *Drosophila*, which is triggered by Gram-positive bacteria and fungi [43]. Pathway activation results in the transcription of antimicrobial peptides such as *defensin* in response to Gram-positive bacteria, and *drosomycin* and *metchnikowin* against fungi [43]. The lysine-type peptidoglycan of Gram-positive bacteria is recognized by three extracellular recognition proteins: peptidoglycan recognition protein SA (PGRP-SA), peptidoglycan recognition protein SD (PGRP-SD), and Gram-negative bacteria binding protein 1 (GNBP1). The $\beta$-glucan constituent of fungal cell wall is recognized by

Gram-negative bacteria binding protein 3 (GNBP3) [43]. Upon recognition of Gram-positive bacteria, GNBP1 hydrolyzes Gram-positive peptidoglycan residues and presents them to PGRP-SA [44]. The signal from these recognition proteins is relayed through a cascade of proteases beginning with modular serine protease (ModSP), then via Gram-positive–specific serine protease (Grass), which finally activates Spz-processing enzyme (SPE) [45]. SPE then cleaves the inactive Spatzle (Spz) precursor, which releases the C-terminal Spz domain [46]. The active Spz dimerises and binds to the transmembrane Toll receptor, which triggers a conformational change and relays the signal inside the cell [43].

The activated Toll receptor recruits the death domain (DD) complex consisting of MyD88, Tube (ortholog of human IRAK4), and Pelle (ortholog of human IRAK1) proteins, which bind to the Toll receptor via the intracellular TIR domains [47]. Tube-Pelle transduces the signal by phosphorylating the *Drosophila* I$\kappa$B factor Cactus. Degradation of Cactus as a result of this phosphorylation leads to the release of the NF-$\kappa$B transcription factor Dif/Dorsal, which enters the nucleus [48]. Like other NF-$\kappa$B proteins, Dif/Dorsal binds to $\kappa$B containing recognition sequences at the promoters of immune response genes such as AMPs and promotes their transcription [43].

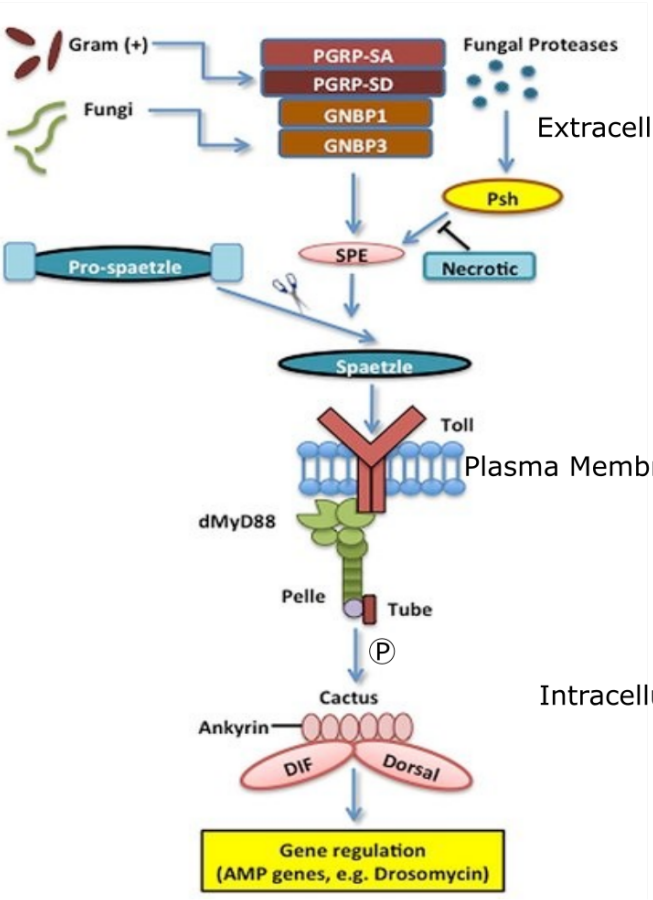



**Figure 1.3: The *Drosophila* Toll signalling pathway**
The *Drosophila* Toll signalling pathway allows recognition of Gram positive bacteria. Upon interaction with pathogen associated molecules, PGRP-SA together with GNBP1 and PGRP-SD activate SPE via a cascade of proteases. SPE cleaves inactive Spatzle which binds and activates Toll receptor. The activated Toll receptor recruits death domain complex (MyD88, Tube, and Pelle) after which the Tube-Pelle complex phosphorylates and degrades I$\kappa$B factor Cactus (containing ankyrin-repeat domains). This frees the NF-$\kappa$B protein Dif/Dorsal, which translocate into the nucleus and trigger transcription of antimicrobial peptides. Figure adapted from Stokes *et al.,* (2015) [49]

In order to understand the role of innate immune pathways Toll and IMD in shaping the gut microbiota, Mistry *et al.,* (2017) performed 16S sequencing on immune-deficient *dif-key* and immune active *pirk;trbd* mutant flies, and compared their gut microbiome to control flies [34]. Dif is the Toll signalling pathway NF-$\kappa$B transcription factor and key (kenny) is the IKK$\gamma$ homolog, which communicates IMD signal to transcription factor Relish in the IMD pathway [50, 51]. Loss of function in both *dif* and *key* renders the fly immune compromised. Trabid [52] and Pirk [53] are negative regulators of the IMD pathway, mutation of which results in flies with a constitutively active immune system. Immune deficient *dif-key* flies showed a pattern of microbial community development which resembled the aging pattern of a wild type fly, but over a much shorter time scale (ie. accelerated development). Additionally, the gut of *dif-key* flies had an increase in bacterial load, potentially as a result of their compromised immune system. The constitutively active immune mutant (*pirk;trbd*) flies had a microbial composition different from both their genetic background control, and the immune compromised *dif-key* mutants [34].

The gut responses to pathogenic bacteria are well understood, however little is known about how the immune signalling pathways distinguish between commensal and pathogenic bacteria. Theoretically, the presence of commensal bacteria in the mucosal layer should result in the constitutive activation of innate immune Toll and IMD pathways. However, this would lead to an al-

teration of the indigenous bacterial composition, and subsequent abrogation of host functions, thereby negatively effecting health [7–12]. To prevent this, the host must carefully regulate AMP expression, to eliminate pathogens without damaging commensals [54, 55]. Disruption of this delicate regulatory mechanism results in a indiscriminate elimination of microbes, leading to dysbiosis.

The importance of Caudal, a negative regulator of AMP production, was shown by Ryu *et al.,* (2008). The group observed that silencing *caudal* resulted in an upregulation of AMPs together with a shift in the dominant bacterial species from *Commensalibacter intestini* to *Gluconobacter morbifer* [54, 55]. An additional regulatory protein Nubbin was described by Dantoft *et al.,* (2013), who reported that loss of NF-$\kappa$B/Relish activity repressor Nubbin resulted in the overexpression of AMPs, even in the absence of infection. Loss of Nubbin also led to a significant reduction of the gut microbial density [56]. Another protein PIMS (PGRP-LC-interacting inhibitor of Imd signalling), a negative regulator of PGRP-LC belonging to the IMD pathway, was found to be expressed in the presence of commensal gut bacteria. Absence of PIMS resulted in the excessive production of AMPs in response to resident gut microbiota [53]. These observations provoke speculation that levels of Caudal and Nubbin may also be regulated by gut microbiota in order to reduce AMP levels and protect themselves from host immune response.

### 1.2.2 Relationship between diet, metabolism and gut microbiota

Individual dietary components such as sugars, triglycerides, and amino acids have also been shown to have an influence in shaping the gut microbiota. Whon *et al.,* (2017) observed that a high sugar diet resulted in dysbiosis of the gut microbiota with a significant increase in *Gluconobacter morbifer* and a decrease in *Commensalibacter intestini* [57]. Moreover, Wong *et al.,* (2014) demonstrated that commensal gut bacteria promoted protein nutrition allocation and repressed carbohydrate/lipid storage in flies fed with a high sugar diet [37].

Flies fed a high fat diet showed an increase in relative abundance of commensal bacteria together with a rise in *C. intestini* levels [58] [59]. Furthermore, Newell *et al.,* (2014) proposed a negative correlation between the abundance of *Acetobacter* and triglyceride levels in the *Drosophila* gut [60]. This was experimentally demonstrated by analysing axenic (germ-free) flies, which were found to have elevated levels of triglycerides and glucose. Mono-colonization of these germ free flies with *Acetobacter* restored the levels of triglycerides and glucose as compared to control flies [60]. A similar observation was reported by Huang *et al.,* (2015), in which mono-colonization of flies with *Acetobacter tropicalis* resulted in a decline of lipid content as compared to uncolonized axenic flies. This decline was in accordance with the consumption of dietary sugars in the food by *Acetobacter tropicalis* [61].

The importance of microbes in harvesting amino acids from a low protein diet was shown by Yamada *et al.,* (2015), in which a fungal symbiont *Issatchenkia orientalis* present in wild flies was found to extend lifespan of malnourished flies by providing amino acids to the host [62]. Moreover, the presence of *Acetobacter pomorum* and *Lactobacilli* in the host was sufficient to buffer the lack of amino acids in a protein deficient diet, and to regulate the protein appetite of the fly [63]. *Acetobacter pomorum* was also shown to restore larval growth in poor protein diets, which was attributed to its ability to stimulate the insulin signalling pathway in the host through interaction with acetic acid producing enzyme pyrroloquinoline quinone–dependent alcohol dehydrogenase (PQQ-ADH) [64].

Commensal gut microbes have also shown to influence host metabolism. Modulation of host metabolism is regulated to a major extent by short chain fatty acids (SCFA) produced by commensal microbes in the gut [65]. Administration of the SCFA, butyrate, to obese mice feeding on a high fat diet prevented development of insulin resistance and obesity [66]. Furthermore, the presence of SCFA acetate led to a reduction of total serum triacylglycerols and cholesterol levels in rats fed with a cholesterol-rich diet [67]. Propionate and butyrate produced by gut bacteria were also found to play a role in intestinal gluconeogenesis, which protected the host from diet-induced obesity and glucose intolerance [68]. Studies in *Drosophila* conducted by Shin *et al.,* (2011) also demonstrated that acetate produced by *Acetobacter pomorum* ac-

tivated the insulin/insulin-like growth factor signalling (IIS) pathway which could explain restoration of larval growth on protein-poor diets [64].

Promotion of growth and development [57, 64], modulation of metabolites [37] and alterations in behaviour [63] are a few downstream host responses which seem to be dependent on alteration of microbial communities due to dietary factors. Both upstream factors and downstream responses in the above studies can be linked to the mTOR pathway.

**The mTOR pathway mediates host metabolism**

The Mammalian Target of Rapamycin (or mTOR) is a serine/threonine kinase which belongs to the family of PI3K-related kinase (PIKK). The 289kDa kinase mTOR comprises of a C terminal FATC domain, kinase domain, FRB (FKBP-rapamycin binding) domain, FAT domain, and 20 HEAT tandem repeats [69]. mTOR functions as a catalytic subunit of the protein complexes mTORC1 and mTORC2 [69], which mediate cellular responses such as growth, protein synthesis, lipid and glucose metabolism, and autophagy. It carries out these functions in response to upstream cues including growth factors, insulin, amino acids, oxygen, and energy levels, through a complex series of interactions [70].

**The mTOR complex 1**

In humans, mTORC1 is composed of three core and two inhibitory subunits [71]. The core subunits of mTORC1 are mTOR kinase, mammalian lethal with Sec13 protein 8 (mLST8), and regulatory-associated protein of mTOR (Raptor). The complex also has two inhibitory subunits: Proline-rich Akt substrate of 40 kDa (PRAS-40) and DEP domain containing mTOR interacting protein (DEPTOR). mLST8 associates with the mTOR kinase domain through an LBE domain at the C lobe [72]. This association indirectly influences the active site by stabilizing the LBE structure involved in the kinase activation loop [72]. Raptor plays an essential role in the lysosomal localization of mTOR complex 1 and forms a nutrient sensitive complex with mTOR [73]. Furthermore, Raptor is reported to shuttle the binding of mTORC1 complex to TOR signalling motifs (TOS) within target proteins, eg. 4E-BP1 and S6K1 [73]. Activated mTORC1 phosphorylates negative regulators PRAS40 and Deptor, thereby reducing their interaction with mTORC1 [74]. The activity of the mTORC1 complex can be regulated by the drug rapamycin. Rapamycin is isolated from *Streptomyces hygroscopius*, and mediates the interaction of FKBP12 with the FRB domain of mTOR. Binding of rapamycin results in the partial obstruction of the active site of mTOR kinase domain in the mTORC1 complex, which partially inhibits its activity [71].

### The mTOR complex 2

The mTOR complex 2 (mTORC2) comprises of mTOR, mLST8, and Rapamycin insensitive companion of mTOR (Rictor) as its core components. It also has the negative regulatory subunits Deptor, mSin1, and Protor1/2 [75]. mTORC2 is regulated by the insulin/PI3K pathway. In the absence of insulin, mTORC2 activity is inhibited by mSin 1 [75]. mTORC2 is also known to phosphorylate Akt and members of the AGC family of protein kinases, and plays an important role in cell survival and proliferation [76].

This study will consider the role of mTORC1 in metabolism **(Figure 1.4)**, and how this protein complex may affect the gut microbiome of *Drosophila*.

### Upstream signalling of mTORC1

Detection of amino acid levels and subsequent regulation of mTORC1 is carried out by Rag GTPases and a ragulator-based lysosomal signalling system. Amino acids activate Rag resulting in exchange of bound GDP with a GTP. This induces the binding of Raptor to the Rag-Ragulator complex, which results in the translocation of mTORC1 to the Raptor subunit on the lysosome. mTORC1 associated with the lysosome is activated by binding to Rag and Rheb GTPases [77, 78].

mTORC1 is also regulated by insulin levels. In the presence of high blood glucose levels, insulin binds and activates the insulin receptor tyrosine kinase. This results in PI3K-induced phosphorylation of phosphatidylinositol

4,5 bisphosphate (PIP2) to generate triphosphate (PIP3) in the presence of insulin receptor substrate 1. PIP3 acts as a secondary messenger, and plays an important role in the recruitment and activation of Akt. Activated Akt phosphorylates and inactivates negative regulators of mTOR TSC1/2 and PRAS40, thus promoting mTORC1 activity [70] **(Figure 1.4)**.

In addition to amino acids and insulin, mTORC1 also responds to cellular energy and oxygen levels through the metabolic regulator AMP kinase. Reduction in cellular energy (increased AMP/ATP ratio) or oxygen levels activates AMP kinase which phosphorylates TSC1/2, thereby inhibiting mTORC1 activity [79]. It is important to note that difference in the amino acid residues of TSC1/2 which are phophorylated by AMPK (Ser1387 and Thr1271) and Akt (Ser939 and Thr1462) results in its activation/inactivation respectively [80]. AMP kinase can also regulate mTORC1 activity by directly phosphorylating Raptor. Moreover, the TSC complex can be activated by low oxygen levels via induction of REDD1 (Regulated in DNA damage and Development 1) [79].

**Downstream targets of mTORC1**

eIF4E Binding Protein (4E-BP) and p70S6 Kinase 1 (S6K1) are two main regulators of protein synthesis and ribosomal biogenesis [81]. 4E-BP inhibits the assembly of the translation initiation complex by binding to elF4E [81]. Activated mTORC1 phosphorylates 4E-BP and reduces its binding

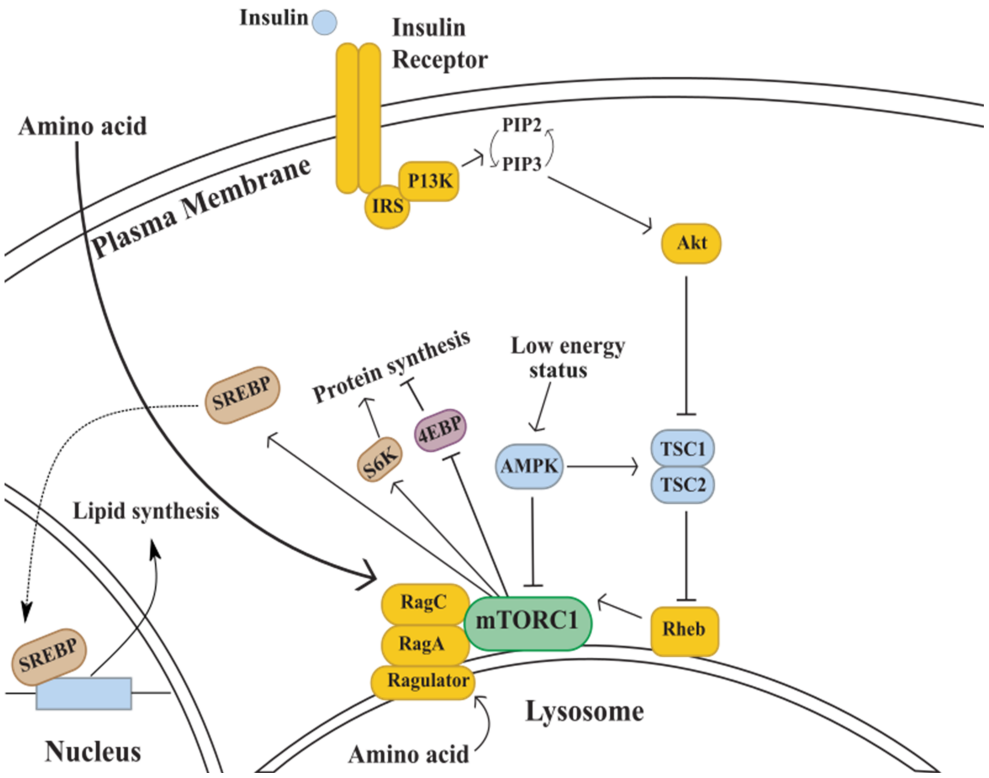



**Figure 1.4: The mTOR pathway** is a master regulator of many cellular processes and drives cells towards anabolism. Its activity is regulated by a variety of upstream cues such as energy status of the cell (AMP:ATP), amino acid levels, and insulin levels. High levels of AMP in the cell activate AMP kinase which phosphorylates TSC1/2 and thereby inhibits mTORC1 activity. Changes in amino acid levels regulate mTORC1 activity via the Rag-Ragulator complex. Additionally, insulin levels also exert control on the activity of mTORC1 through the PI3K/Akt pathway. In response to upstream cues, mTORC1 promotes lipid and protein synthesis through regulating activity of proteins S6K, 4E-BP and SREBP. Dissociation of phosphorylated 4E-BP from elF4E in response to activation by mTORC1 results in initiation of 5'cap-dependent mRNA translation through elF4E activity. S6K1 protein kinase is phoshorylated by mTORC1 which promotes ribosomal biogenesis and hence protein translation. Finally the SREBP group of transcription factors activated by mTORC1 promote transcription of genes involved in fatty acid synthesis. Modified illustration of the mTOR pathway in mammals adapted from Saxton *et al.*, (2017) [79].

affinity with elF4E, resulting in its dissociation and consequent initiation of 5'cap-dependent mRNA translation [81]. Phosphorylation of S6K1 kinase by mTORC1 results in promotion of mRNA translation through phosphorylation of intermediate substrates [81]. Therefore, 4E-BP and S6K1 play an important role in the regulation of cellular protein levels [81].

mTORC1 is also known to regulate cellular lipid levels by promoting lipid synthesis and regulating lipolysis [82]. Lipid synthesis is positively regulated by mTORC1 through activation of Sterol Regulatory Element Binding Protein (SREBP) transcription factors. This results in the transcription of genes involved in fatty acid and cholesterol synthesis [82]. SREBP can also be activated by phosphorylation of SREBP inhibitory protein Lipin 1 or through the S6K1 mediated pathway [82]. Lipolysis or breakdown of lipids is negatively regulated by mTORC1 through reduction in the expression of adipose triglyceride lipase (ATGL) and hormone-sensitive lipase (HSL), which catalyzes the breakdown of triglycerides [82].

mTORC1 promotes glycolysis and the oxidative pentose phosphate pathway by promoting expression of several pathway-specific enzymes, and thereby facilitates cell growth. Increased levels of transcription factor HIF1$\alpha$ as a result of mTORC1 activation, facilitates the expression of glycolytic enzymes including phospho-fructo kinase (PFK) [83]. Furthermore, mTORC1 mediated SREBP activation promotes the transcription of glucose 6-phosphate dehydrogenase (G6PD) - a rate limiting enzyme in the pentose phosphate

pathway [79]. Activated SREBP also promotes production of NADPH, ribose, and other intermediate metabolites of the pentose phosphate pathway by increasing its flux [79]. These metabolites provide energy and substrates for the synthesis of lipids and nucleotides, and thus facilitate cell proliferation and growth [79, 83].

**The *Drosophila* metabolic mTOR pathway**

The mTOR pathway is highly conserved amongst eukaryotes [79, 84]. *Drosophila* TOR (dTOR) shares 56% sequence homology with human mTOR at the protein level. Of this, the FRB and kinase domains are the most conserved [85]. dTOR has been extensively studied for its role in growth and development of *Drosophila*, using TOR mutants or by treating flies with rapamycin [86] [87]. In one such study, Teleman *et al.,* (2005) showed that upregulation of d4EBP activity induced by rapamycin treatment resulted in an in-vivo increase in fat reserves [88]. Other components of the *Drosophila* TOR pathway are homologous to those in the mammalian mTOR pathway such as dTsc1/2, dRheb, d4EBP, dS6K, and dRagA/C proteins [89–92].

There are a few studies which links gut dysbiosis, diet, and the mTOR pathway. Mice fed with soybean meal (SBM) protein diet showed a variation in the gut microbiome with a high abundance of Bacteroidales family. In addition to this, regulatory genes related to the mTOR pathway (such as *lck* and *fyn* genes) were affected, together with a decline in phosphorylated

mTOR levels in these mice [93]. Mice fed with a high fat diet exhibited microbial dysbiosis, and had an increase in levels of FOXO3 and Akt phosphorylation (FOXO3 and Akt are associated with the mTOR pathway) [94]. In another study, growth promoting effects of gut microbiota, especially *Lactobacillus plantarum* in *Drosophila* larvae feeding on poor nutrient food was attributed to TOR-dependent hormonal growth signalling via insulin receptor and ecdysone signalling pathways [95].

Based on these studies, we hypothesise that the mTOR pathway could be involved in mediating host-diet-microbe relationship in *Drosophila*.

### 1.2.3 Interaction between immunity and metabolism

Multiple studies have shown diet and immunity to be the two major factors that shape the gut microbiota [34, 64, 96]. However, only a few studies have reported a clear interaction between these two biological processes in determining the composition of the gut microbiota.

The mTORC1 inhibitor rapamycin has been of a great interest to the scientific community, due to its immune suppressive and anti-aging properties. Fan *et al.,* (2015) demonstrated that rapamycin treatment increases the levels of negative regulators of the IMD pathway including Caudal, USP36, and PGRPs-SC, and delays expansion of microbiota in aging *Drosophila* guts [97]. Furthermore, a study conducted by Schinaman *et al.,* (2019) showed that rapamycin treatment in *Drosophila* reduced the levels of *Alphaproteobacteria*

and promoted lifespan extension that was independent of the presence of gut microbiome [98].

Another protein of interest shown to affect both the metabolic and immune response in *Drosophila* is the *Drosophila* homologue of 4E-BP protein *thor*, a downstream target of mTORC1 [99]. Bernal *et al.,* (2000) showed that the *thor* gene contains GATA sequences in its promoter, which serve as binding site for NF-$\kappa$B. The group also demonstrated that Thor was upregulated in response to infection, and that *thor* mutants had similar phenotypes to those of immune compromised flies, thereby indicating its importance in host defence [99].

## 1.3 Aims of the study

Many studies have provided interesting insights on the dysregulation of host-microbe interactions mediated by metabolic and/or immune pathways in *Drosophila*. The dysbiosis observed in disease raises questions on how the innate immune system and metabolism interact with each other to shape the gut microbiome. Additionally, a secreted bacterial recognition protein PGRP-LB$^{PC}$ was recently shown to play a role in preserving the intestinal microbiota, making it interesting to speculate on the interaction between the extracellular PGN recognition protein PGRP-SA of the Toll signalling pathway and commensal bacteria [100].

This thesis addresses two key questions:

**1) Is the Toll signalling pathway receptor protein PGRP-SA involved in the preservation of commensal gut bacteria?**

**2) Does mTORC1 inhibitor rapamycin affect the composition of the gut microbiota in PGRP-SA mutant flies?**

This work should help us understand the effect of both innate immune signalling (Toll signalling pathway) and metabolism (mTOR pathway) on the composition of the *Drosophila* gut populations.

# 2 Materials and Methods

## 2.1 *Drosophila* stocks, and genetics

Yellow white (*yw*) *Drosophila* strain $YW^{67c23}$, $W^{1118}$, and DGRP (*Drosophila* Genetic Reference Panel) *25174* were used as genetic backgrounds for performing assays, and preparing genetic immune and metabolic mutants. In this study, site specific knockdowns were prepared by using the UAS-GAL4 system. In this technique, site specific GAL4 transcription factor drives upstream activating sequence (UAS) tagged with an RNAi sequence to produce knockdowns. *Drosophila* strains used in this study are enlisted in **Table 2.1** along with their source and a brief description.

## 2.2 *Drosophila* husbandry

During the experiments, flies were reared at 25°C, 70% humidity, on standard cornmeal-molasses medium **(Appendix 5.1:*Drosophila* media recipe)** under a 12 hour light and 12 hour dark cycle. Backup stocks for each line were maintained at 18°C. Experimental flies were allowed to mate for two days after collection in vials with fresh fly food. They were then segregated based on sex into separate vials. Around 15 to 20 flies of the same sex were housed in each vial for every experiment and tipped into fresh food every two days till 30 days.

| Genotype | Source | Description |
|---|---|---|
| $W^{1118}$ | Bloomington (RRID:BDSC_3605) | Flies have a loss of function mutation of *w* in gene CG2759 resulting in white eyes. |
| *yw* | Bloomington (Bl≠6599 Y[1] w[67,23]) | Flies in this line have a point mutation in the *y* gene at the X chromosome resulting in its characteristic yellow body color. |
| *yw seml* | [101] | Flies have a loss of function point mutation in *pgrp-sa* gene at the X chromosome. |
| *yw* $dif^1$ | [51] | Flies have a point mutation in *dif* gene at 2L chromosome resulting in loss of DIF function. |
| *25174;Cyo-GFP/IF;TM3S6/25174* | Bloomington (RRID:BDSC_25174) | *Drosophila* genetic background prepared by Huang *et al.,* [102] |
| *25174 seml* | Lab stock | Flies in this line have a point mutation in *pgrp-sa* gene in 25174 genetic background. |
| *25174* $dif^1$ | Lab stock | Flies in this line have a point mutation in *dif* gene in *25174* genetic background. |
| $GNBP1^{osi}$ | [103] | Flies in this line have an insertional mutation in *gnbp1* gene. |
| *UAS* $mTOR^{RNAi}$ | Bloomington (A15495 TRiP line(II)) | Flies contain an RNAi of serine threonine kinase mTOR coupled with a UAS region. |
| *UAS* $4EBP^{RNAi}$ | VDRC 100739, Vienna | Flies contain an RNAi of 4E-BP coupled with a UAS region. |
| *UAS* $AMPK^{RNAi}$ *(II)* | VDRC 106200, Vienna | Flies contain an RNAi of AMP Kinase, coupled with a UAS region. |
| *UAS* $PGRP\text{-}SA^{RNAi}$ | VDRC line 37470 (GD), Vienna | Flies contain an RNAi of PGRP-SA coupled with a UAS region. |
| *yw seml; Cyo-GFP/UAS* $mTOR^{RNAi}$ | Lab stock | Flies contain a UAS RNAi of mTOR and *pgrp-sa* mutation in *yw* background. |
| *yw seml; CyoGFP/UAS* $4EBP^{RNAi}$ | Lab stock | Flies contain a UAS RNAi of 4E-BP and *pgrp-sa* mutation in *yw* background. |
| *yw seml; Cyo-GFP/UAS* $AMPK^{RNAi}$ | Lab stock | Flies contain a UAS RNAi of AMPK and *pgrp-sa* mutation in *yw* background. |
| *NP1-GAL4/Cyo; drsGFP/TM3* | Bloomington (RRID:BDSC_67088) | Flies contain an enterocyte specific GAL4 driver. |

**Table 2.1:** *Drosophila melanogaster* strains used in this study.

Rapamycin (37094, Sigma-Aldrich, USA) stock (10mg/ml) was freshly prepared in 100% ethanol and added into microwaved fly food to a final concentration of 200$\mu$M. The same amount of ethanol (1:50 dilution) was also added to fly food as a vehicle control [84]. Flies were fed with Rapamycin food for three days after which their guts were isolated for different experiments.

## 2.3 Characterization of the *Drosophila* gut microbiota

### 2.3.1 Culture dependent quantification of gut microbiota

Individual *Drosophila* midguts were dissected in Phosphate-buffered saline (PBS) solution and then homogenized in De Man, Rogosa and Sharpe (MRS) broth (CM0359, Oxoid,Thermo Fisher, USA) **(Appendix 5.2: MRS media recipe)** using a sterile needle. The resulting suspension was then plated on MRS agar (CM0361, Oxoid,Thermo Fisher, USA), and incubated at 30°C for 48 hours. The colonies in each plate were counted, and $\log_{10}$ values of the colony forming units (CFU's) were calculated. Five to fifteen individual guts of a particular fly line were plated on individual MRS plates and the same steps were performed. The $\log_{10}$ CFU values of mutants and controls were statistically compared using student's t-test, and graphs were plotted in GraphPad Prism v.8.0.

### 2.3.2 Culture independent identification of gut microbiota

The identification of microbial families is widely performed by analysing their 16s ribosomal RNA sequences. The 16S sequences are comprised of nine hypervariable regions (V1-V9) which are flanked by conserved sequences [104]. In this study, we sequenced the hypervariable region V3 to identify microbial composition of the *Drosophila* gut.

**DNA isolation and processing**

Forty midguts were isolated from 5 day and 30 day old flies of each strain in PBS, and their genomic DNA (gDNA) was extracted using QIAamp DNA Mini Kit (51304, Qiagen, Germany) according to manufacturer's instructions. A no gut sequencing control was also included to rule out any contaminant bacteria in the reagents.

Readout of the composition of *Drosophila* microbiome is challenged by the intra-cellular endosymbiont *Wolbachia*, which is known to infect *Drosophila* [105]. To remove/reduce the 16S reads of *Wolbachia*, the extracted DNA was digested with the restriction enzyme BstZ17I (R3594S, NEB, UK) which cuts at a unique restriction site in the 16S region of *Wolbachia* RNA only [105].

Approximately 500ng of genomic DNA (gDNA) from each fly line was incubated with BstZ17I for 2 hours **(Figure 2.1)**, followed by heat inactivation of the enzyme. The digested gDNA was then used as a template

to amplify the 16S hypervariable regions V1-V3 using primers given in **Table 2.4**. This amplification step was carried out with Phusion HF DNA polymerase (MO530L, NEB, UK) by applying the PCR conditions given in **Table 2.2**. *Wolbachia* 16S region are not amplified during this step, due to the aforementioned digestion, resulting in a higher yield of amplicons of the gut microbiota. Digestion of the V1-V3 region of *Wolbachia* after PCR amplification of its 16S gDNA resulted in the production of a 200bp and 300bp bands, both of which were confirmed to belong to *Wolbachia*through sequencing **(Figure 2.1, lane 2)**. The Qiagen PCR Purification Kit (27106, Qiagen, Germany) was used to purify the PCR products, which was then used as a template to amplify V3 hypervariable region (180-200bp). The primer sequences and thermal conditions used to amplify V3 region with Phusion HF polymerase (MO530L, NEB, UK) are detailed in **Table 2.4 and 2.3** respectively. After amplification, the resulting V3 product was run on a 1.2% agarose gel, and a 200bp V3 band was excised and purified using the QIAquick Gel Extraction Kit (28706, Qiagen, Germany).

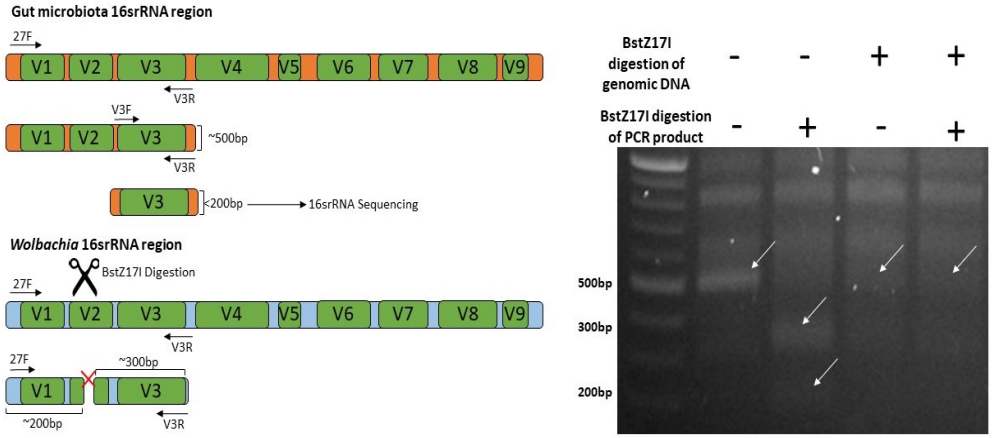



**Figure 2.1: Wolbachia 16S DNA digestion assay**
Agarose gel image showing V1-V3 PCR product of *Drosophila* gut microbiome digested with BstZ17I before and after amplification of V1-V3 16S regions. Lane 1 is - -, Lane 2 is - + (two bands: 300bp, 200bp represents the digested *Wolbachia* V1-V3 region), Lane 3 is + - and Lane 4 is + +. PCR products after digestion in lane 2 (300bp, 200bp) were confirmed to belong to *Wolbachia* through sequencing.

## V3 library preparation

Upto 100ng of V3 DNA samples (measured using Picogreen assay (P11496, Thermo Fisher, USA) according to manufacturer's instructions) were used for library preparation. The NEBNext®Fast DNA library Prep Set for Ion Torrent$^{TM}$ kit (E6270, NEB, UK) was used to prepare DNA libraries. The NEB end repair enzyme from the kit was utilized to remove DNA overhangs and ensure that each DNA molecule contains a free 5' phosphate and 3' hydroxyl groups for adaptor ligation. This was carried out using the reaction mix and thermocycling conditions according to manufacturer's instructions. Unique Ion Xpress$^{TM}$ Barcode Adaptors (4471250, ThermoFisher Scientific, USA) along with universal adaptors supplied in the kit were then ligated to

| Temperature | Duration | Number of cycles |
|---|---|---|
| 98°C | 30 seconds | 1 cycle |
| 95°C | 30 seconds | 35 cycles |
| 65°C | 30 seconds | |
| 72°C | 1 minute | |
| 72°C | 5 minutes | 1 cycle |

**Table 2.2:** PCR cycling conditions used to amplify hypervariable regions 1-3 (V1-V3) from BSTZ17I (R3594S, NEB, UK) digested *Drosophila* gut gDNA. Amplification was performed using phusion polymerase (MO530L, NEB, UK).

| Temperature | Duration | Number of cycles |
|---|---|---|
| 98°C | 30 seconds | 1 cycle |
| 95°C | 30 seconds | 35 cycles |
| 66°C | 30 seconds | |
| 72°C | 15 seconds | |
| 72°C | 5 minutes | 1 cycle |

**Table 2.3:** PCR cycling conditions used to amplify hypervariable region 3 (V3) from V1-V3 16S template. Amplification was performed using phusion polymerase (MO530L, NEB, UK).

the ends of the DNA strands and amplified according to manufacturer's instructions. The resultant DNA libraries were then purified using Agencourt AMPure XP DNA purification beads (A63881, Beckman Coulter, Germany) to remove excess barcodes from the product. Samples were run on 2% E-gel (G661012, ThermoFisher Scientific, USA) using the SizeSelect 2% setting (E-Gel iBase Invitrogen) and 300bp libraries were extracted and purified twice using Agencourt AMPure XP DNA purification beads (A63881, Beckman Coulter, Germany). The purified libraries were then amplified using 6-8 rounds of PCR and quantified with the KAPA library quantification kit

| Primer ID | Sequence | Template |
|---|---|---|
| **16S_27Fw** | 5'-AGAGTTTGATCCTGGCTCAG-3' | V1-V3 |
| **V3_Fw** | 5'-CCAgACTCCTACGGGAGGCAG-3' | V3 |
| **V3_Rv** | 5'-CGTATTACCGCGGCTGCTG-3' | V1-V3, V3 |
| **IT_A** | 5'-CCATCTCATCCCTGCGTGTC-3' | V3 library |
| **IT_tr_P1** | 5'-CCACTACGCCTCCGCTTTCCTCTCTATG-3' | V3 library |

**Table 2.4:** Primers used to amplify 16S hypervariable regions V1-3 (16S_27Fw, V3_Rv), V3 (V3_Fw, V3_Rv) and quantify V3 DNA libraries (IT_A,IT_tr_P1).

for Ion Torrent$^{TM}$ (KK4812, KAPA Biosystems, USA) using primers mentioned in **Table 2.4** against Ion Torrent$^{TM}$ DNA standards (KK4812, KAPA Biosystems, USA). Samples were then mixed equally to a final concentration of 350pM, loaded onto the Ion 314$^{TM}$ Chip V2 using Ion Chef$^{TM}$ system, and sequenced using Ion Proton$^{TM}$ system, (ThermoFisher Scientific, USA) according to manufacturer's instructions.

The Ion Proton$^{TM}$ system works under the principle of sequencing by synthesis. In this method, identification of nucleotide bases are performed by tracking changes in the pH. Formation of a phosphodiester bond during dNTP polymerization leads to the release of protons, which can be detected as a pH change. The Ion Torrent$^{TM}$ system detects these changes in the pH using ISFET (Ion sensitive field effect transistor) detectors placed in each micro-well. Signals from millions of ISFET detectors are relayed through CMOS array chips, which presents the nucleotide readout [106] **(Figure 2.2)**.

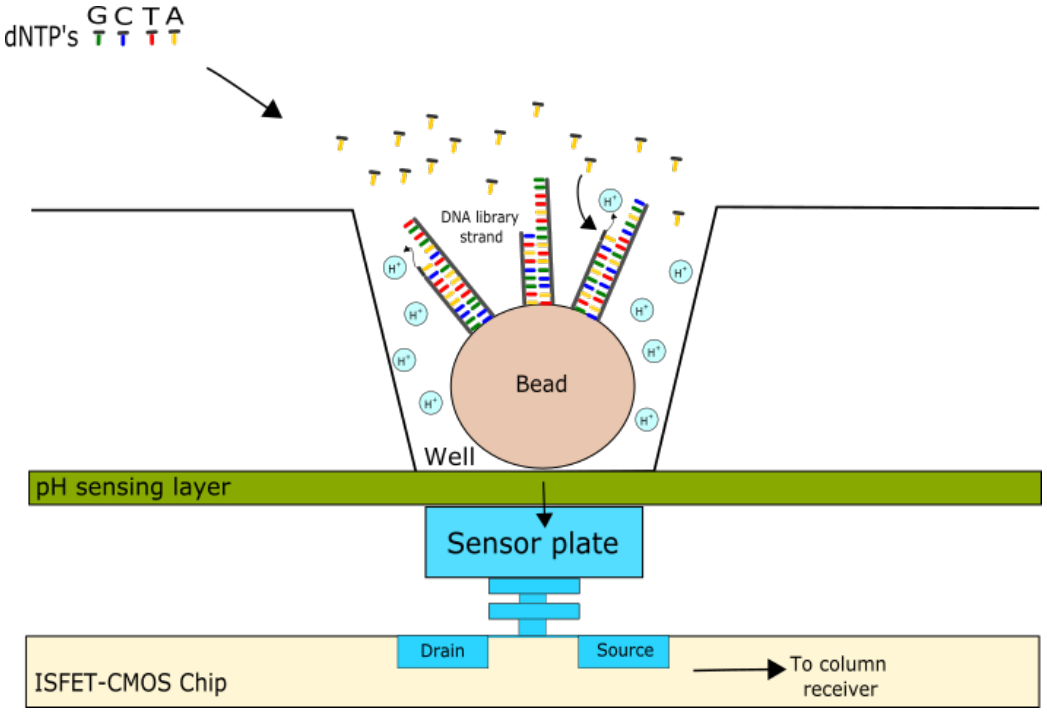



**Figure 2.2: Principle of ion torrent sequencing**
Single nucleotides are added to the Ion $314^{TM}$ Chip V2 containing DNA libraries ligated to beads. These nucleotides bind to the DNA strand based on nucleotide complementarity and release a hydrogen ion. Release of protons, results in a change of the pH of the well. This change is detected by the sensor plates, which is converted into digital signal by ISFET detectors. The digital signals are then relayed through the silicon chip and are presented as nucleotide readouts.

**Sequence analysis**

The sequencing data produced by the Ion Proton$^{TM}$ system was processed using the ThermoFisher Scientific Ion Reporter$^{TM}$ software. Sequences were uploaded as BAM files and analyzed using a standard designed metagenomics 16S workflow version 5.10 (Thermo Fisher, USA) with V3 primers mentioned in **Table 2.4** and customized parameters as described later. The sequences were referenced against Curated MicroSEQ(R) 16S Reference Library v2013.1. Reads were filtered so that single end primers were detected in every read, sequences less than 115 bp were excluded from the results, and all reads that would align with at least 90% of the database sequence were included. Operational taxonomic Unit (OTU) with at least one unique read was picked up. Cutoffs at 97% and 99% sequence identity were used for assignment at genus and species levels respectively. The difference between two consecutive hits was set at 0.8%. Reads mapping to the sequences of the *Drosophila* symbionts belonging to Anaplasmataceae (which do not constitute members of the gut microbiome), were excluded from the downstream analysis. The relative abundance of each family was estimated by dividing mapped reads from each family by the total mapped reads (minus Anaplasmataceae) per sample.

The diversity of microbiota within and between each sample was measured by plotting alpha (Simspn's 1-D, and Shannon H) and beta diversity (PCA plot) indices respectively using PAST3 software [107]. Alpha diversity takes

into account both species richness and abundance within the same study. Simpson's and Shannon's indices are commonly used to score the alpha diversity of a population. Simpson's index (D) measures the probability of selecting two individuals from a population belonging to the same species, while Shannon's diversity index (H) measures the species richness and evenness in terms of uncertainty of predicting species in a sample (ie. entropy) [108]. Beta diversity analysis, compares the bacterial composition between sample populations and plots a representative Principle component analysis (PCA) plot. Distance between points in the PCA plots represents the extent of similarity/dissimilarity between samples based on their composition [109]. All graphs in these experiments were produced in GraphPad Prism v.8.0. PCA plots were prepared in the PAST3 software and edited using Inkscape v.0.92.4.

## 2.4 Lifespan analysis

Prior to carrying out lifespan assay, *yw*, *yw seml* and *yw dif*$^{1}$ flies were backcrossed for two generations to remove any inbred mutations. Two day-old mated female flies were collected in batches of 10 per vial in 12 vials (120 per fly line). These flies were tipped into fresh food every 2 days until all the flies died. Survival was monitored by counting the number of dead flies every alternate day. Unaccounted flies that flew off during tipping or died because of manual handling were recorded as censored. The number of dead and censored flies were tabulated in a custom excel template designed by Matthew

Piper (Monash University, Australia) which was used to produce the lifespan graph. Lifespan of two different fly strains were statistically compared using Log-rank test in which the difference between two populations at a time point is examined by analyzing the probability of an event (death) to occur [110].

## 2.5 Measuring gene expression in *Drosophila*

### 2.5.1 RNA isolation

Ten flies from each line were dissected in PBS and their midguts were isolated. These guts were then homogenized, and total RNA was extracted using Norgen total RNA purification plus kit (48400, Norgen-Biotek, Canada). The RNA concentration (50-500 ng/$\mu$l) and purity (260nm/280nm absorbance ratio) was measured using Nanodrop. The absorbance ratio of RNA (260nm) and proteins (280nm) indicates the purity of RNA in the sample. For one single fly line, RNA was isolated from a pool of 10 guts. This was performed three times per fly line.

### 2.5.2 cDNA preparation

Total RNA was used as a template to prepare cDNA using the SuperScript™ VILO™ cDNA Synthesis Kit (11754050, Thermo Fisher, USA) based on manufacturer's instructions.

### 2.5.3 Quantitative PCR

qPCR was performed using cDNA produced from total RNA (described above) of fly guts as template. The SensiFAST™ SYBR®No-ROX Kit (BIO-98020, Bioline, Germany) and sequence specific primers **(Table 2.5)** were used to quantify transcript levels of 4E-BP against the housekeeping gene RP49 with the help of the Qiagen Rotor gene Q qPCR instrument. The amount of cDNA added was standardized to 25ng/$\mu$l of the precursor RNA. Quantification was performed according to manufacturer's instructions. I have not demonstrated that RP49 is stable in different experimental conditions in this project, however, literature shows that RP49 has been commonly used as a housekeeping gene in studies involving immune mutant flies [34, 52, 111].

| **Primer ID** | **Sequence** | **Template** |
|---|---|---|
| **4E-BP_Fw** | 5'-GCCCATGATCACCAGGAAG-3' | 4E-BP |
| **4E-BP_Rv** | 5'-CCCGCTCGTAGATAAGTTTGG-3' | 4E-BP |
| **Rp49_Fw** | 5'-CCAGTCGGATCGATATGCTAA-3' | Rp49 |
| **Rp49_Rv** | 5'-GTTCGATCCGTAACCGATGT-3' | Rp49 |

**Table 2.5:** Primers used to quantify 4E-BP (4E-BP_Fw, 4E-BP_Rv) and Rp49 (Rp49_Fw, Rp49_Rv) mRNA levels.

### 2.5.4 Analysis of qPCR data

$\Delta C_T$ values were obtained by subtracting the $C_T$ values of 4E-BP from the $C_T$ values for an internal control ribosomal protein Rp49. These values were then used to estimate the relative fold change of 4E-BP transcript levels in

mutants against their genetic backgrounds by calculating the $\Delta\Delta C_T$ value [112, 113]. The equation for calculating the $\Delta\Delta C_T$ is given below:

$$\text{TE-TC}=\Delta C_T exp$$

(TE is Tested Experimental $C_T$ value and TC is gene being Tested Control $C_T$ value).

$$\text{HE-HC}=\Delta C_T cont$$

(HE is Housekeeping gene Experimental $C_T$ value and HC is Housekeeping gene Control $C_T$ value).

$$\Delta C_T exp\text{-}\Delta C_T cont=\Delta\Delta C_T$$

$$R_{FC}=2^{-\Delta\Delta CT}$$

($R_{FC}$ is Relative Fold Change)

Three biological repeats were each loaded in triplicates (three technical repeats) (n=9) and $\Delta\Delta C_T$ values were plotted and analysed for statistical significance using student's t-test in GraphPad Prism v.8.0.

# 3 Results

## 3.1 Loss of PGRP-SA changes cultivable microbial density in young flies

Extracellular bacterial recognition protein PGRP-SA recognizes Gram positive bacterial peptidoglycan and activates the Toll signalling pathway, which leads to the production of antimicrobial peptides [31]. These recognition proteins have been well studied for their interaction with pathogenic Gram positive bacteria (eg. *Staphylococcus aureus*, *Streptococcus faecalis*, *Bacillus thuringiensis*, and *Micrococcus luteus*) [101], but their influence on commensal bacteria have not been well described. Hence, we wanted to first investigate the role of PGRP-SA in affecting the commensal bacteria of the *Drosophila* gut using *seml* mutation [101]. To test this, we analysed the cultivable gut microbial load of female *yw seml* and *yw* flies at different ages (larval stage, as well as 5 and 30 day old adult flies). We observed a significant decrease in the cultivable gut microbial load ($\log_{10}$ CFU's) of 3rd instar *yw seml* mutant larvae (n=5) as compared to their genetic background (*yw*) larvae (n=5) (p-value = 0.0317). A similar decline was also observed in the guts of 5 day old *yw seml* flies (n=10) (student's t-test p-value = 0.0014). However, 30 day old *yw seml* (n=10) flies did not show a significant difference in the cultivable microbial load (student's t-test p-value = 0.2085) **(Figure 3.1)**.

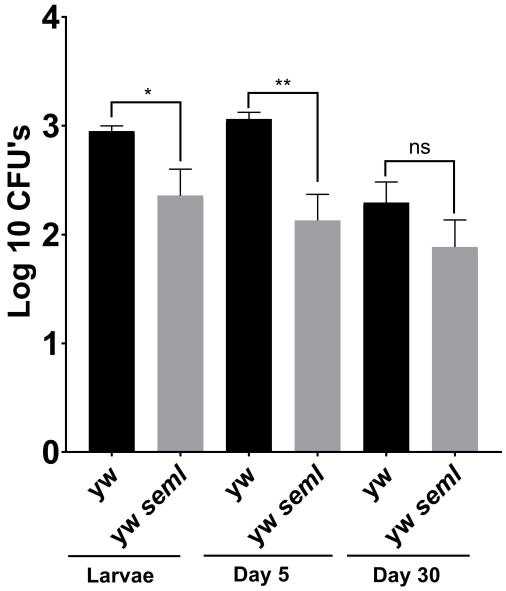



**Figure 3.1: PGRP-SA influences cultivable microbial load in young *Drosophila* gut.**
The graph represents the cultivable gut microbial load of larvae (n=5), 5 day old (n=10) and 30 day old (n=10) female *yw*, and *yw seml* flies. The x axis represents fly strains at different ages and y axis represents $\log_{10}$ CFU's (ns = not significant, *p $\leq$ 0.05, **p $\leq$ 0.01, ***p $\leq$ 0.001, ****p $\leq$ 0.0001).

To investigate the role of the genetic background in the loss of cultivable microbial load, we plated *25174 seml* mutants that have the same *seml* mutation as *yw seml* but in a DGRP *25174* genetic background. Upon comparison, we found that young female DGRP *25174* flies carrying *seml* (n=10) mutations also had a significantly reduced cultivable microbial load as compared to their genetic background control (n=10) (student's t-test p-value = 0.0007). This reduction was in accordance with the observed differences in young female *yw seml* mutant flies, confirming that the loss of cultivable

microbiota in *seml* mutants is independent of their genetic background **(Figure 3.2)**.

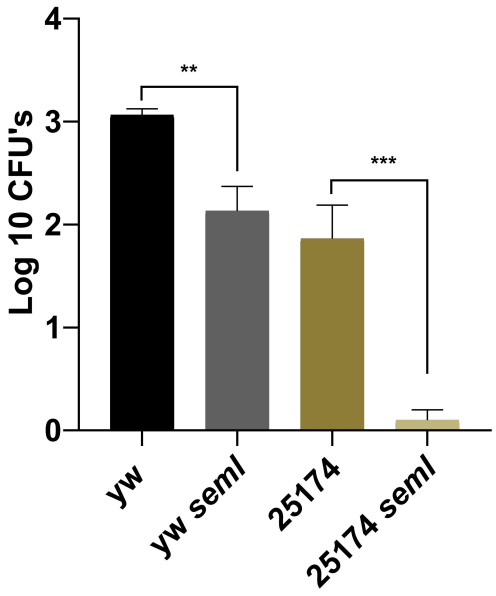



**Figure 3.2: Loss of cultivable microbial load is independent of their genetic background in *seml* mutant flies.**
The graph represents the cultivable gut microbial load of 5 day old female *yw*, *yw seml*, *25174*, *25174 seml* flies. The x axis represents 5 day old fly strains of two different genetic backgrounds *yw* and *25174* (DGRP) and y axis represents $\log_{10}$ CFU's, n=10 (ns = not significant, *p $\leq$ 0.05, **p $\leq$ 0.01, ***p $\leq$ 0.001, ****p $\leq$ 0.0001).

Commensal bacteria are compartmentalized in the mucosal layer of the gut, which consists of extracellular bacterial recognition proteins and AMPs secreted by the gut epithelium [114–117]. Thus, we sought to assess if PGRP-SA secreted by the epithelial cells (enetrocytes) interacts and influences the commensal microbial load in the mucosal layer. We tested this by performing a site specific knockdown (RNAi) of PGRP-SA in the enterocyte cells (NP1-

GAL4) which line the gut of *Drosophila*. Similar to the whole mutant *seml* flies, enterocyte specific PGRP-SA$^{RNAi}$ (n=10) also resulted in a significant reduction in the load of cultivable gut microbiota (student's t-test p-value $<$ 0.0001) **(Figure 3.3)**.

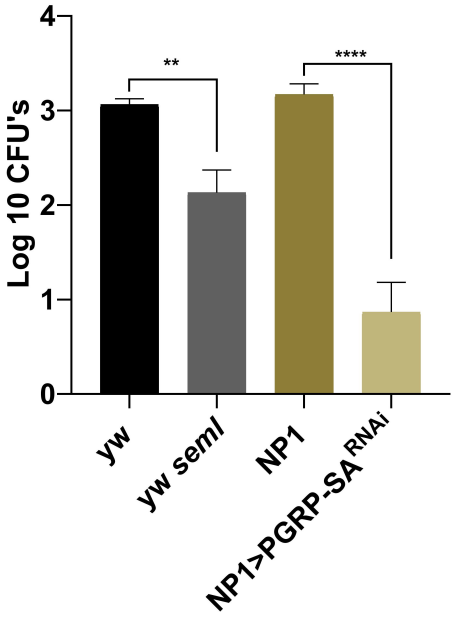



**Figure 3.3: PGRP-SA produced in the enterocyte cells of the gut influences cultivable microbial load in young *Drosophila***
The graph represents the cultivable gut microbial load of 5 day old female *yw*, *yw seml*, NP1-GAL4 (enterocyte cell GAL4 driver), and NP1>PGRP-SA$^{RNAi}$ (RNAi of PGRP-SA in Enterocyte cells) flies. The x axis represents 5 day old fly strains and y axis represents $\log_{10}$ CFU's, n=10 (ns = not significant, *p $\leq$ 0.05, **p $\leq$ 0.01, ***p $\leq$ 0.001, ****p $\leq$ 0.0001).

## 3.2 PGRP-SA associated protein GNBP1 also influences cultivable microbial density in flies

Extracellular protein GNBP1 is known to associate, process and present bacterial PGN to PGRP-SA, leading to the activation of the Toll signalling pathway [44]. Its association with PGRP-SA and processing of bacterial PGN made us speculate about its interaction with commensal gut bacteria. To assess the contribution of GNBP1 in influencing the cultivable gut bacteria, we plated *GNBP1*$^{osi}$ whole mutants developed in the $w^{1118}$ genetic background. A significant decline of the cultivable microbial load was observed in the guts of young *GNBP1*$^{osi}$ mutant female flies (n=10), as compared to their genetic background ($w^{1118}$ flies) (n=10) (student's t-test p-value = 0.0007) **(Figure 3.4)**. However, this cultivable microbial load increased in 30 day old *GNBP1*$^{osi}$ mutant female flies (n=5) (student's t-test p-value = 0.0238) **(Figure 3.4)**. This suggested that *GNBP1*$^{osi}$ also contributes in influencing the cultivable microbial load of the *Drosophila* gut

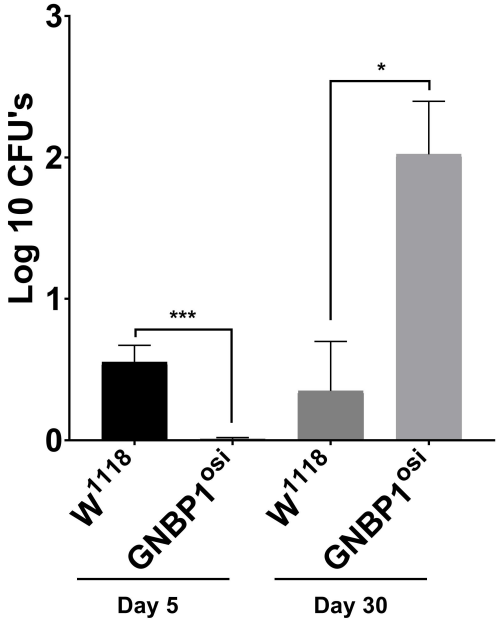



**Figure 3.4: Gram-negative bacteria binding protein 1 (GNBP1) influences cultivable microbial load in guts of 5 and 30 day old *Drosophila***
The graph represents the cultivable gut microbial load of 5 day old (n=10) and 30 day old (n=5) $w^{1118}$, and $GNBP1^{osi}$ female flies. The x axis represents different fly strains of different ages, and y axis represents $\log_{10}$ CFU's, (ns = not significant, *p $\leq$ 0.05, **p $\leq$ 0.01, ***p $\leq$ 0.001, ****p $\leq$ 0.0001).

## 3.3 The NF-$\kappa$B homologue DIF influences cultivable bacteria in the *Drosophila* gut

After establishing that bacterial recognition proteins PGRP-SA and GNBP1 influences the cultivable gut microbial load of young flies, we wanted to test the effects of downstream NF-$\kappa$B (DIF) on the indigenous bacteria of the gut.

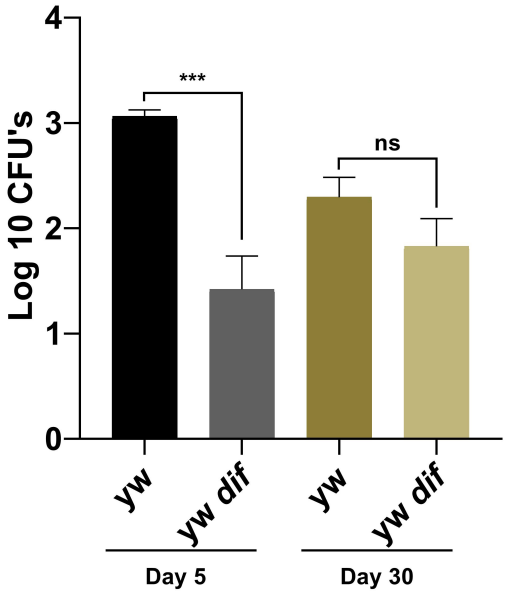



**Figure 3.5: DIF influences cultivable microbial load in young *Drosophila* gut** The graph represents the cultivable gut microbial load of 5 day old and 30 day old female *yw*, and *yw dif*$^{1}$ flies. The x axis represents fly strains at different ages and y axis represents $\log_{10}$ CFU's. n=5 (5 day old *yw dif*$^{1}$), n=10 (all others) (ns = not significant, *p $\leq$ 0.05, **p $\leq$ 0.01, ***p $\leq$ 0.001, ****p $\leq$ 0.0001).

Guts from *dif*$^{1}$ whole mutant adults of ages 5 and 30 days, were used to analyze the cultivable gut microbial load. We observed that functional loss of DIF led to a significant reduction in the cultivable gut microbial load of 5 day old female flies (n=5) (student's t-test p-value = 0.0007) **(Figure 3.5)**. A similar result was also observed in *dif*$^{1}$ mutants constructed in *25174* (DGRP) genetic background (n=10) (student's t-test p-value = 0.0019) **(Figure 3.6)**. However, in 30 day old female flies, loss of DIF did not seem to effect the cultivable microbial load of the gut (n=10) (student's t-test p-value = 0.1689) **(Figure 3.5)**. Similarity in the trend of the age dependent loss of commensal

microbial load in both *seml* and *dif*$^{1}$ mutant flies suggested that members of the canonical Toll signalling pathway are involved in shaping the *Drosophila* gut microbiome.

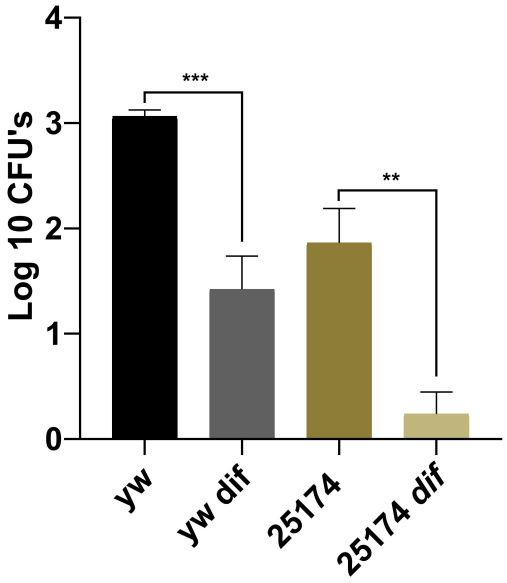



**Figure 3.6: Loss of cultivable microbial load is independent of the genetic background in *dif*$^{1}$ mutant flies.**
The graph represents the cultivable gut microbial load of 5 day old female *yw* (n=10), *yw dif*$^{1}$ (n=5), *25174* (n=10), and *25174 dif*$^{1}$ (n=10) flies. The x axis represents 5 day old fly strains of two different genetic backgrounds *yw* and *25174* (DGRP) and y axis represents $\log_{10}$ CFU's, (ns = not significant, *p $\leq$ 0.05, **p $\leq$ 0.01, ***p $\leq$ 0.001, ****p $\leq$ 0.0001).

## 3.4 Young PGRP-SA mutant flies lack Lactobacillaceae

We next performed 16S rRNA high-throughput DNA sequencing to further elucidate the influence of PGRP-SA on the composition of the commensal bacterial species in the *Drosophila* gut. The relative abundance of bacterial families detected in the gut of female *yw* and *yw seml* flies (n=40 guts/strain)

(5 and 30 day old) are shown in **Figure 3.7**. Guts of young 5 day old female *yw* flies were dominated by Lactobacillaceae (48%) and Acetobacteraceae (23%) along with the presence of Rhodobiaceae, Propionibacteriaceae and many other bacterial families (others $\approx$ 30%). Dominance of Lactobacillaceae in the gut of young flies correlated with previous studies [28]. In contrast to this, young 5 day old female *yw seml* mutant flies had a substantially reduced abundance of Lactobacillaceae, which accounted to only 0.6% of the total gut microbiome. This reduction in Lactobacillaceae was also observed in its biological repeat **(Supplementary Figure 5.1)**. Furthermore, the relative abundance of Acetobacteraceae in *yw seml* mutant flies increased to 63% of the total gut microbiome and the remaining 36% encompassed other bacterial families **(Figure 3.7)**.

Similar to the 5 day old microbial composition, 30 day old female *yw* flies also showed a dominance of Lactobacillaceae (47%) and Acetobacteraceae (15%). Interestingly, a 10-fold increase in the relative abundance of the bacterial family Nocardioidaceae was observed in 30 day old female *yw* flies (20%) as compared to their 5 day old counterparts (2%). Thirty day old *yw seml* flies on the other hand showed a substantial increase in Lactobacillaceae (43%), which turned out to be the most abundant family of the microbiome followed by Acetobacteraceae (22%) **(Figure 3.7)**.

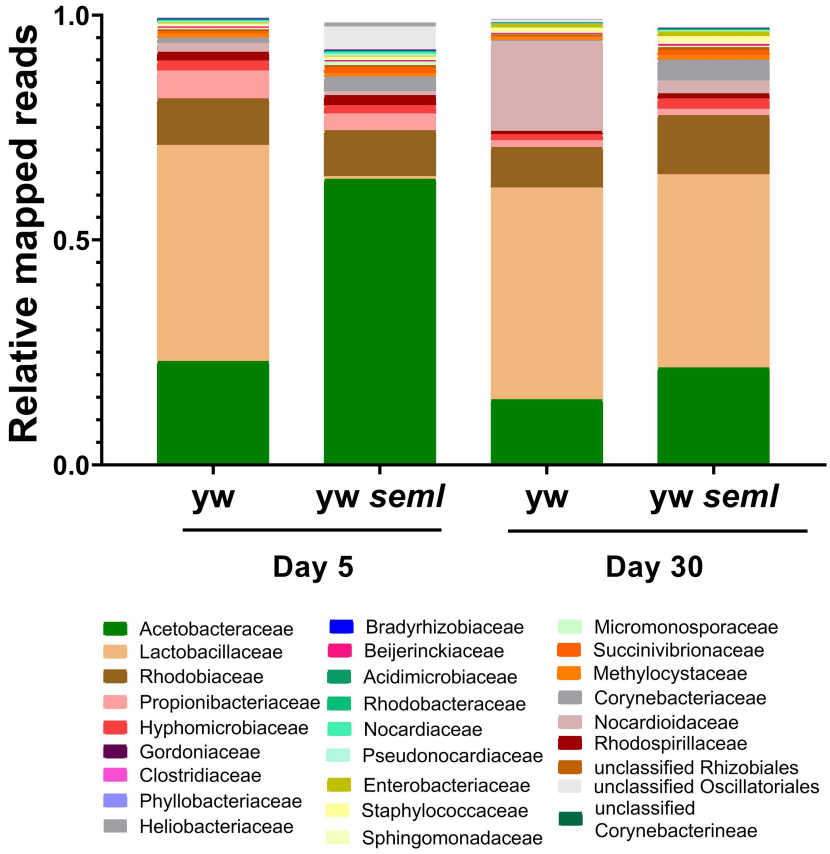



**Figure 3.7: Effect of loss of PGRP-SA in the gut microbial composition of 5 and 30 day old flies.**
The graph represents the relative abundance of microbial families observed in the gut of 5 day and 30 day old female *yw*, *yw seml* flies revealed by 16S next-generation sequencing. The x axis represents fly strains of different ages, and the y axis represents relative mapped reads. (n=40 guts/strain).

Statistical tests for Alpha and Beta diversity were performed to assess the diversity of the microbiome within and between fly lines **(refer Section 2.3.2: sequence analysis)**. Approximately 116 bacterial families were recorded ($S_{obs}$) in young *yw* flies, which remained almost the same as the flies

aged to 30 days ($\approx$ 117 families). Similarly, the number of bacterial families reported in young *yw seml* flies ($\approx$ 149 families) remained almost the same as *yw seml* flies aged to 30 days ($\approx$150 families) **(Figure 3.8 C)**. Alpha diversity measurements revealed that the 5 day old *yw seml* flies (Simpson 1-D = 0.5768, Shannon H = 1.499) were less diverse than *yw* flies (Simpson 1-D = 0.7004, Shannon H = 1.673). However, as the flies reached 30 days old, the microbiota of *yw seml* flies (Simpson 1-D = 0.7465, Shannon H = 1.864) became more diverse than that of *yw* flies (Simpson 1-D = 0.7086, Shannon H = 1.627) **(Figure 3.8 A,B)**. Variation in the dominant Acetobacteraceae levels with age in *seml* mutant flies could be the reason for this diversity pattern. The *yw* flies showed no such change in the diversity pattern across these two ages as seen in **(Figure 3.8 A,B)**. This could be due to a similar relative abundance pattern and almost same $S_{obs}$ between 5 and 30 day old flies.

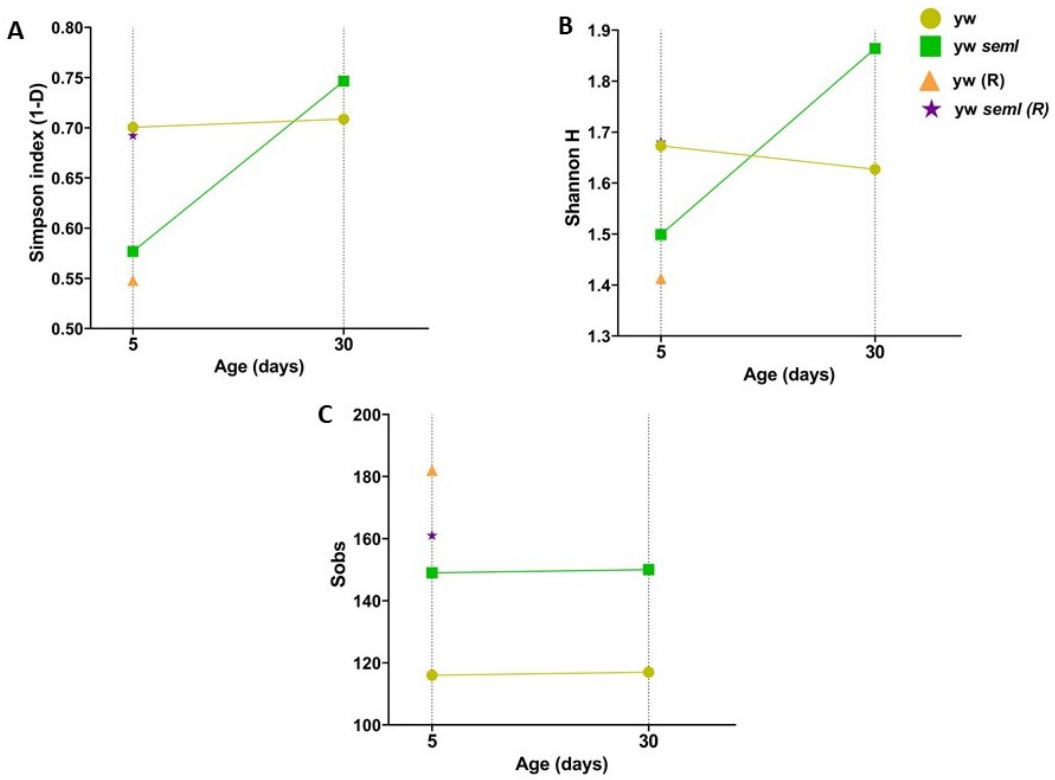



**Figure 3.8: Alpha diversity analysis of *yw* and *yw seml* flies of different ages (5 and 30 day).**
The graphs represent alpha diversity indices of female *yw* and *yw seml* across two ages (5 and 30 days). (A) Simpson's (1-D) index, (B) Shannon H index an (C) Total number of bacterial families observed ($S_{obs}$). R represents biological repeat. (n=40 guts/strain)

.

Beta diversity analysis is performed to examine the differences in the bacterial composition between individual fly lines. Principal component analysis (PCA) is a tool to understand differences in multidimensional space and is commonly used to measure the beta diversity of microbial communities in *Drosophila* [32, 34, 118]. Beta diversity analysis (PCA plot) confirmed that

*yw* and *yw seml* clustered far apart in both 5 and 30 day old flies, which indicated that they were dissimilar to each other. Interestingly, 30 day old *yw seml* flies appeared to be similar to their 5 day old genetic background (*yw*) as shown in the PCA plot **(Figure 3.9)**. This could be because both these flies share almost the same levels of the dominant families of Acetobacteraceae (*yw seml* 30 day = 22%, *yw* 5 day = 23%) and Lactobacillaceae (*yw seml* 30 day = 43%, *yw* 5 day = 48%) as well as the remaining reads (*yw seml* 30 day = 35%, *yw* 5 day = 29%) were constituted by the same number of families (23 families).

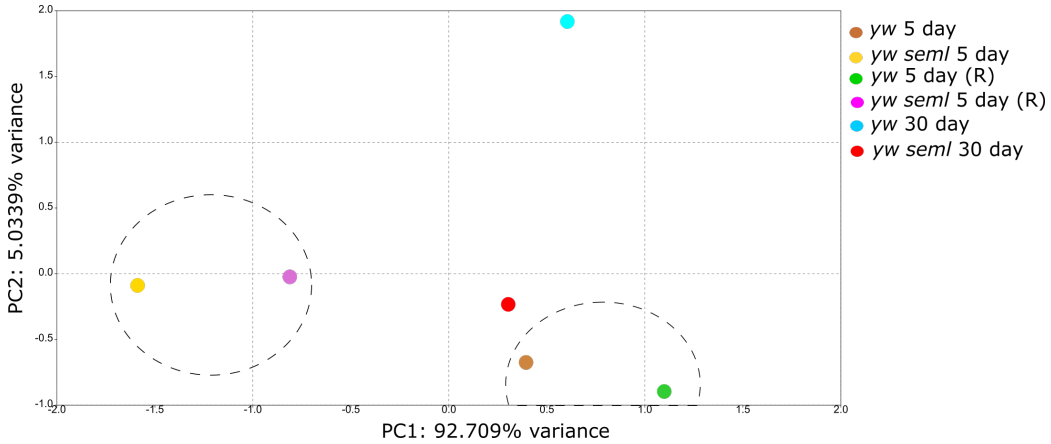



**Figure 3.9: Principal component analysis (PCA) of *yw* and *yw seml* flies of different ages (5 and 30 day).**
The graph represents PCA plot (Beta diversity) of female *yw* and *yw seml* across two ages (5 and 30 days). R represents biological repeat.(n=40 guts/strain).

## 3.5 Rapamycin does not effect the microbial diversity of young *seml* mutant flies

Dietary nutrients such as sugars [37, 119], amino acids [64, 93] and triglycerides [61, 94] have been shown to shape the gut microbiota. In some of these studies, dietary factors are linked to the change in microbial composition via alterations in the mTOR pathway [93–95, 119].

To test if variation in the host metabolism had any effect on the bacterial composition of *seml* flies, we altered the activity of the protein kinase mTOR. In this study, we inhibited its activity by either genetically silencing mTOR in the gut of *seml* flies (*yw seml;NP1>mTOR*$^{RNAi}$) or by pharmacologically inhibiting it using rapamycin. We also treated *yw seml;NP1>mTOR*$^{RNAi}$ flies with rapamycin to address its side effects in the absence of mTOR. Bacterial families were sequenced by performing 16S rRNA high-throughput DNA sequencing (n=40 guts/strain) and analyzed using alpha and beta diversity statistical tests. All sequencing experiments of the above mentioned fly lines were compared with *yw* and *yw* + Rap respectively and were performed in both young (5 day old) and middle aged (30 day old) flies.

**Effect of Rapamycin on the gut microbiota of young *Drosophila***

Rapamycin treatment of young (5 day old) female *yw* and *yw seml* flies resulted in a shift in the relative abundance of different bacterial families as shown in **Figure 3.10**. In *yw* flies, rapamycin treatment led to a 3-fold

reduction of Lactobacillaceae (48% in *yw* versus 17% in *yw* + Rap), 3-fold increase of Acetobacteraceae (23% in *yw* versus 70% in *yw* + Rap) and a 10-fold decrease of Propionibacteriaceae (6% in *yw* versus 0.6% in *yw* + Rap). Approximately 118 and 116 bacterial families ($S_{obs}$) were reported in rapamycin treated and untreated *yw* flies respectively **(Figure 3.11 C, 5 days)**. Alpha diversity analysis revealed that treatment of *yw* flies with rapamycin reduced the diversity of the gut microbiota (*yw*: Simpson 1-D = 0.7004, Shannon H = 1.673; *yw* + Rap: Simpson 1-D = 0.4785, Shannon H = 1.107) **(Figure 3.11 A,B, 5 days)**. Dissimilarity of the bacterial composition between *yw* and *yw* + Rap was confirmed by analyzing the PCA plot **(Figure 3.12)**. These results suggested that rapamycin had an effect on the microbial composition and diversity of young *yw* flies.

Furthermore, as shown in **Figure 3.10**, rapamycin treatment did not seem to have a major effect on the relative abundance of microbial families in *yw seml* mutant flies. Both treated and untreated female *yw seml* flies lacked Lactobacillaceae (0.5% and 0.6% respectively) as compared to their genetic background (17% and 48% respectively). Moreover, Acetobacteraceae largely dominated the gut bacteria of both treated and untreated *yw seml* flies (59% and 63% respectively). However, treating *yw seml* flies with rapamycin led to a 6-fold increase in Propionibacteriaceae (*yw seml*: 4% ; *yw seml* + Rap = 24%). Approximately 141 and 149 bacterial families ($S_{obs}$) were reported in both treated and untreated *yw seml* flies respectively **(Figure 3.11C, 5**

**days)**. Simpson's (1-D) and Shannon H indices also showed that rapamycin treatment of *yw seml* flies had very little to no effect on the diversity of the gut microbiota (*yw seml*: Simpson 1-D = 0.5768, Shannon H = 1.499; *yw seml* + Rap: Simpson 1-D = 0.5878, Shannon H = 1.37) **(Figure 3.11A,B, 5 days)**. PCA plot showed that treated and untreated *yw seml* flies clustered far from one another, but the degree of dissimilarity was lesser than that observed between treated and untreated *yw* flies **(Figure 3.12)**. This suggested that rapamycin had very little effect in determining the microbial composition and diversity of young *seml* mutant flies.

We then compared the 16S rRNA sequencing data of rapamycin fed female *yw seml* flies with male *yw seml;NP1>mTOR$^{RNAi}$* flies to check the genetic effect of rapamycin in shaping the gut microbiota. We sequenced male guts of *yw seml;NP1>mTOR$^{RNAi}$* in order to retain the x linked *seml* mutation. NGS data **(Figure 3.10)** showed that both rapamycin treated female *seml* flies and mTOR knocked-down male *seml* flies (*yw seml;NP1>mTOR$^{RNAi}$*) had a somewhat similar microbial composition with an abundant Acetobacteraceae family (63% and 77% respectively) and a highly depleted Lactobacillaceae family (0.61% and 0.86% respectively). However, changes in the relative abundance of Propionibacteriaceae and Nocardioidaceae was observed between these lines. The $S_{obs}$ of young *yw seml* flies treated with rapamycin was $\approx$ 141 families, while young *yw seml;NP1>mTOR$^{RNAi}$* flies reported $\approx$ 105 families **(Figure 3.11 C, 5 days)**. Alpha diversity index measurements

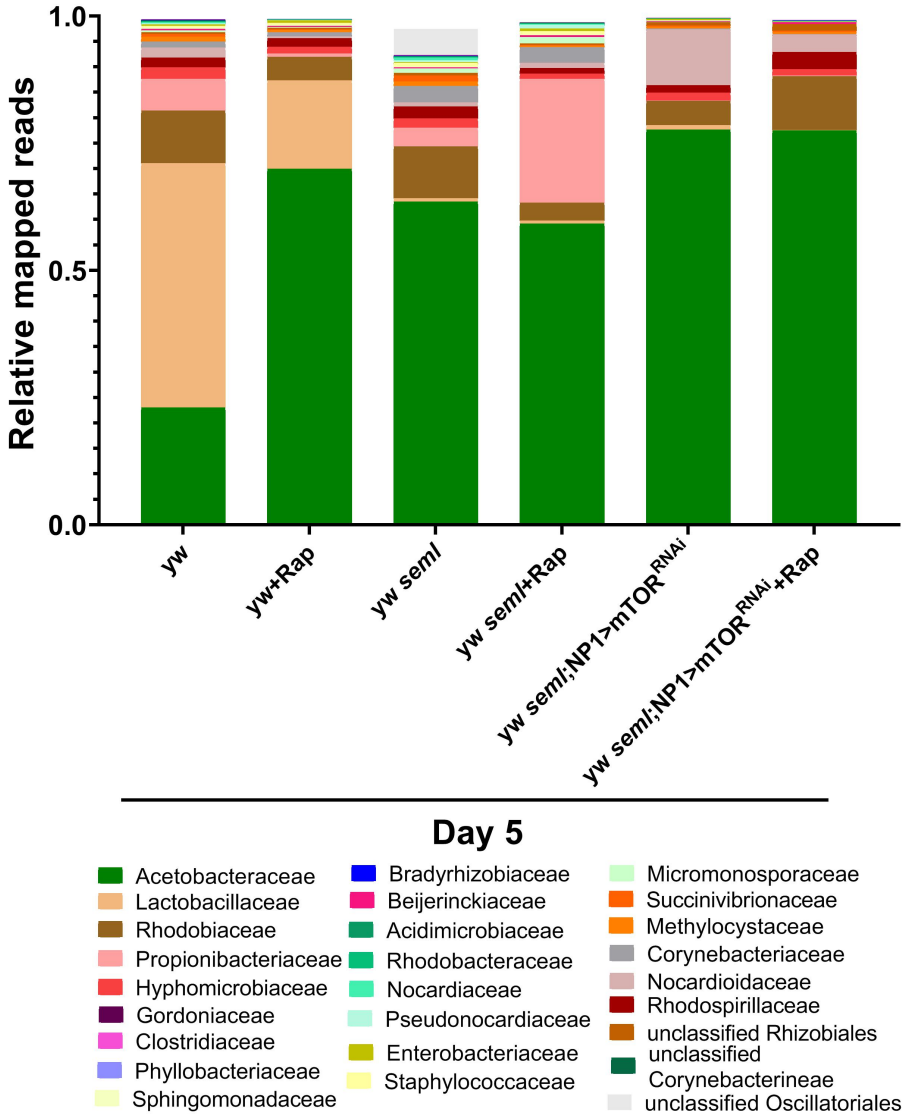



**Figure 3.10: Effect of Rapamycin treatment and gut specific knockdown of mTOR on the microbial composition of 5 day old flies.**
The graph represents the relative abundance of microbial families observed in the gut of 5 day old *yw* (female), *yw seml* flies (female) treated with rapamycin and *yw seml;NP1>mTOR$^{RNAi}$* flies (male) (+/- rapamycin) as revealed by 16S next generation sequencing. The x axis represents fly strains of different ages, and the y axis represents relative mapped reads. (n=40 guts/strain).

revealed that *yw seml* flies treated with rapamycin (Simpson 1-D = 0.5878, Shannon H = 1.37) had a greater diversity as compared to *seml* flies with a silenced mTOR (Simpson 1-D = 0.3825, Shannon H = 0.9148) **(Figure 3.11 A,B, 5 days)**. The PCA plot showed a difference in composition between these two strains **(Figure 3.12)**. A difference in the diversity, and to some extent, the microbial composition could be attributed to the variation in the genetic ($\text{mTOR}^{RNAi}$) versus pharmacological (rapamycin) effect of inhibiting mTOR activity.

Sequencing young male *yw seml;NP1>*$mTOR^{RNAi}$ flies treated with rapamycin showed no major shift in the relative abundance of the dominant family of Acetobacteraceae as compared to their untreated counterpart (*yw seml*;NP1>$\text{mTOR}^{RNAi}$). However slight shifts in the abundance Lactobacillaceae, Rhodobiaceae and Nocardioidaceae was observed, but these shifts did not substantially alter the composition and diversity of the gut microbiota **(Figure 3.10)**. Approximately 126 and 105 bacterial families ($S_{obs}$) were reported in rapamycin treated and untreated *yw seml;NP1>*$mTOR^{RNAi}$ flies respectively **(Figure 3.11 C, 5 days)**. Alpha diversity for *yw seml;NP1>*$mTOR^{RNAi}$ + Rap (Simpson 1-D = 0.386, Shannon H = 0.927) was similar to untreated *yw seml;NP1>*$mTOR^{RNAi}$ (Simpson 1-D = 0.3825, Shannon H = 0.9148) **(Figure 3.11 A,B, 5 days)**. Moreover, beta diversity analysis of the microbial composition of treated and untreated *yw seml;NP1>*$mTOR^{RNAi}$ flies revealed that they were similar as they were closely clustered to each

other **(Figure 3.12)**. Similarities in the microbial profile indicated that rapamycin did not considerably effect the microbial composition in the absence of mTOR, thereby suggesting that rapamycin treatment produced mTORC1 dependent results in young *seml* flies.

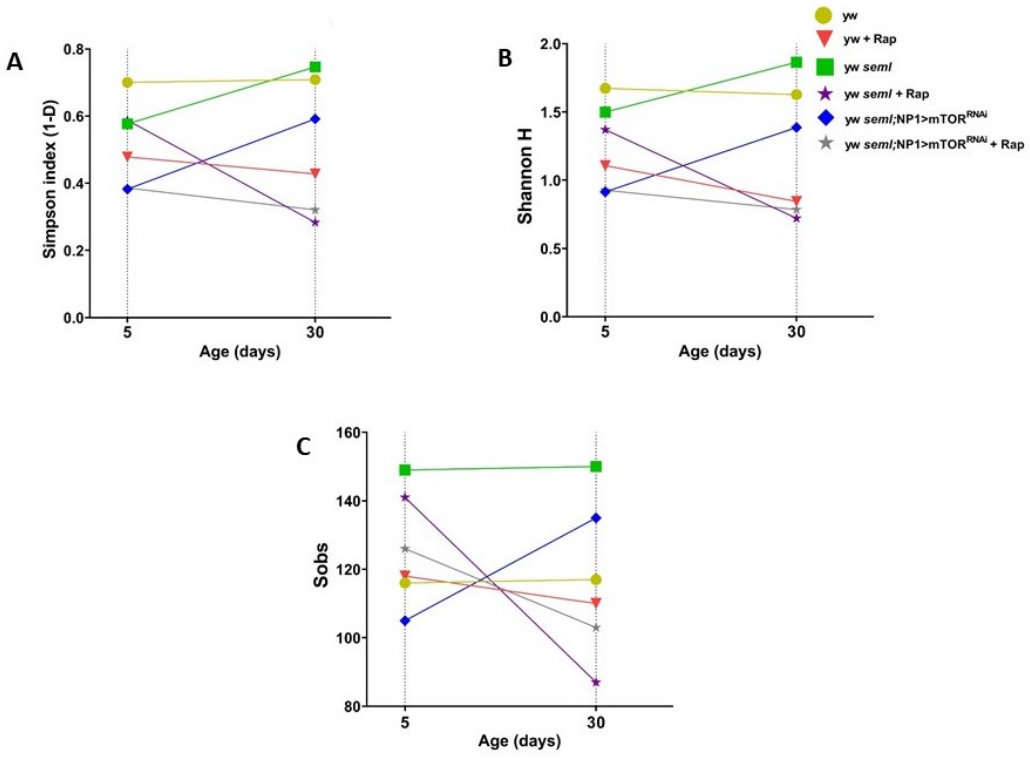



**Figure 3.11: Alpha diversity analysis of 5 and 30 day old flies treated with rapamycin and/or carrying mTOR$^{RNAi}$.**
The graphs represent alpha diversity indices of strains *yw* (female), *yw seml* (female), *yw* + Rap (female), *yw seml* + Rap (female), *yw seml;NP1>mTOR$^{RNAi}$* (male), and *yw seml;NP1>mTOR$^{RNAi}$* + Rap (male) across two ages (5 and 30 days). (A) Simpson's (1-D) index, (B) Shannon H index an (C) Total number of bacterial families observed ($S_{obs}$). (n=40 guts/strain).

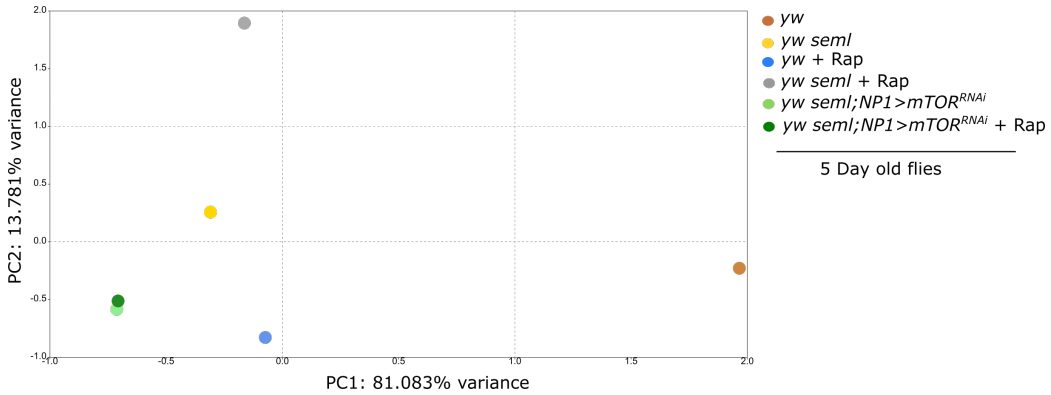



**Figure 3.12: Principal component analysis (PCA) of 5 day old flies treated with rapamycin and/or carrying mTOR$^{RNAi}$.**
The graph represents PCA plot (Beta diversity) of 5 day old fly strains: *yw* (female), *yw seml* (female), *yw* + Rap (female), *yw seml* + Rap (female), *yw seml;NP1>mTOR$^{RNAi}$* (male), and *yw seml;NP1>mTOR$^{RNAi}$* + Rap (male). (n=40 guts/strain).

## Effect of rapamycin on the gut microbiota of middle age *Drosophila*

After establishing the effect of rapamycin in determining the bacterial composition of young flies, we wanted investigate the effects of rapamycin treatment on older flies (30 day old). Transient treatment of 30 day old female *yw* flies with rapamycin resulted in a shift in the microbial composition from a dominant Lactobacillaceae (47%) population in untreated *yw* flies to a dominant Acetobacteraceae population in rapamycin treated *yw* flies (72%). Furthermore, a reduction in other abundant bacterial families such as Rhodobiaceae (9% in *yw* to 2% in *yw* + Rap) and Nocardioidaceae (20% in *yw* to 0.3% in *yw* + Rap) was also observed when *yw* flies were treated with rapamycin **(Figure 3.13)**. The $S_{obs}$ for rapamycin treated and untreated *yw* flies were $\approx$ 110 and $\approx$ 117 families respectively **(Figure 3.11 C, 30 days)**. Similar to their 5 day counterparts, 30 day old rapamycin treated *yw* flies (Simp-

son 1-D = 0.4278, Shannon H = 0.8452) were less diverse as compared to 30 day old untreated *yw* flies (Simpson 1-D = 0.7086, Shannon H = 1.627) **(Figure 3.11 A,B, 30 days)**. Moreover, PCA plot showed a large distance between treated and untreated *yw* strain, which suggested that they were dissimilar, and confirmed that rapamycin treatment resulted in a shift in the microbial composition of 30 day old *yw* flies **(Figure 3.14)**.

Rapamycin treatment of 30 day old female *yw seml* flies resulted in a change in the gut microbial composition, which was mainly marked by a 4-fold increase of Acetobacteraceae (21% in *yw seml* to 85% in *yw seml* + Rap) and a 15-fold decrease of Lactobacillaceae (43% in *yw seml* to 3% in *yw seml* + Rap) **(Figure 3.13)**. Approximately 87 and 150 bacterial families ($S_{obs}$) were reported in rapamycin treated and untreated 30 day old *yw seml* flies respectively **(Figure 3.11 C, 30 days)**. Alpha diversity analysis revealed that rapamycin treatment of 30 day old *yw seml* flies (Simpson 1-D = 0.2836, Shannon H = 0.7219) resulted in a decrease in diversity as compared to untreated *yw seml* (Simpson 1-D = 0.7465 , Shannon H = 1.864) **(Figure 3.11 A,B, 30 days)**. Principle component analysis (PCA) plot further confirmed this result by placing treated and untreated *yw seml* flies far apart from each other **(Figure 3.14)**, which suggested that Rapamycin had an effect on the microbial composition and diversity of 30 day old *seml* flies. This result was contrary to their 5 day old counterpart, in which rapamycin treatment did not have a significant effect on either the composition or on the diversity of

the gut microbiota.

We then compared the relative abundance of *yw seml* flies treated transiently with rapamycin (female) and *seml* flies with gut specific knockdown of mTOR (*yw seml;NP1>mTOR$^{RNAi}$*) (male). *Yw seml;NP1>mTOR$^{RNAi}$* flies showed a microbial composition different from rapamycin treated *seml* flies **(Figure 3.13)**. A dominance of Nocardioidaceae family (60%) was observed in these knockdown mutant flies, while dominance of Acetobacteraceae (84%) was seen in rapamycin treated *seml* flies. Moreover, both fly lines lacked Lactobacillaceae in their gut (3% in *yw seml* + Rap versus 0.4% in *yw seml;NP1>mTOR$^{RNAi}$*) **(Figure 3.13)**. The $S_{obs}$ for 30 day old rapamycin treated *yw seml* flies was $\approx$ 87 and the $S_{obs}$ for 30 day old *yw seml;NP1>mTOR$^{RNAi}$* was $\approx$ 135 families **(Figure 3.11 C, 30 days)**. Alpha diversity measurements revealed that the gut microbiota of 30 day *yw seml;NP1>mTOR$^{RNAi}$* flies (Simpson 1-D = 0.5917, Shannon H = 1.386) was more diverse than *seml* mutants fed with rapamycin (Simpson 1-D = 0.2836, Shannon H = 0.7219) **(Figure 3.11 A,B, 30 days)**. Beta diversity analysis (PCA plot) showed that these two strains clustered far apart from each other, suggesting that they had a dissimilar composition based on the relative abundance of their bacterial families **(Figure 3.14)**. Major differences in the microbial composition and diversity in 30 day old *yw seml;NP1>mTOR$^{RNAi}$* as compared to 30 day old *yw seml* + rapamycin could be due to the reduced levels of mTOR throughout the lifespan in the

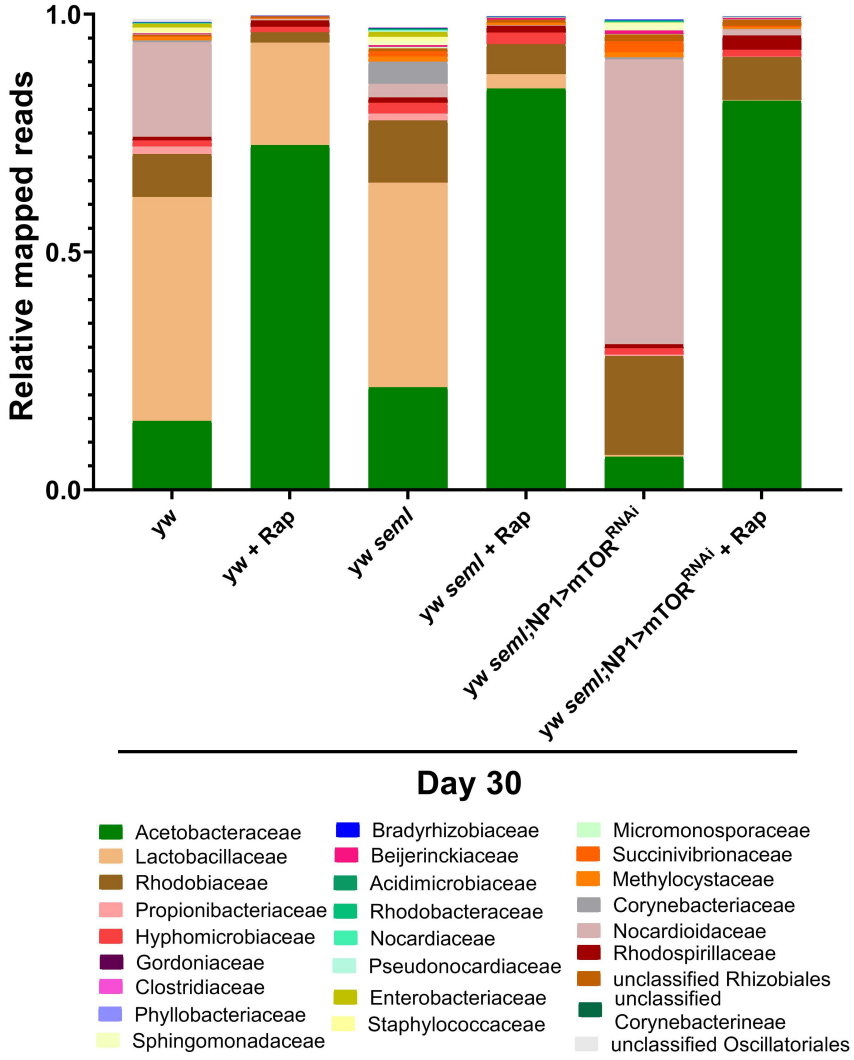



**Figure 3.13: Effect of Rapamycin treatment and gut specific knockdown of mTOR on the microbial composition of 30 day old flies.**
The graph represents the relative abundance of microbial families observed in the gut of 30 day old flies *yw* (female), *yw seml* (female) flies treated with rapamycin and *yw seml;NP1>mTOR*$^{RNAi}$ (male) flies (+/- rapamycin) as revealed by 16S next generation sequencing. The x axis represents fly strains of different ages, and the y axis represents relative mapped reads. (n=40 guts/strain).

former fly line as compared to transient inhibition of mTORC1 in the latter strain.

Lastly, we compared rapamycin treated and untreated male *yw seml*;NP1> $mTOR^{RNAi}$ flies to test the effects of rapamycin on the microbial composition in the absence of mTOR. Relative abundance calculations showed that Acetobacteraceae constituted to about 81% of the gut bacteria in *yw seml;NP1>*$mTOR^{RNAi}$ flies treated with rapamycin. On the other hand, only 7% of the gut microbiota of untreated *yw seml;NP1>*$mTOR^{RNAi}$ flies belonged to Acetobacteraceae. Moreover, Lactobacillaceae was almost absent in both treated anduntreated flies ((+Rap: 0.14%, -Rap: 0.3%). A reduction in the relative abundance of families: Nocardioidaceae (+Rap: 1.3%, -Rap: 60%) and Rhodobiaceae (+Rap: 9%, -Rap: 21%) was also observed in rapamycin treated *yw seml;NP1>*$mTOR^{RNAi}$ flies **(Figure 3.13)**. The $S_{obs}$ for rapamycin treated and untreated mutant flies were $\approx$ 103 and $\approx$ 135 families respectively **(Figure 3.11 C, 30 days)**. Alpha diversity measurements revealed that treating *yw seml;NP1>*$mTOR^{RNAi}$ mutant flies with rapamycin resulted in a decrease in the diversity (+Rap: Simpson 1-D = 0.321, Shannon H = 0.7853; -Rap: Simpson 1-D = 0.5917, Shannon H = 1.386) **(Figure 3.11 A,B, 30 days)**. This difference between treated and untreated mutant flies was also confirmed by beta diversity analysis (PCA plot) in which both were clustered far apart from each other **(Figure 3.14)**. Together, these results indicated that rapamycin had an influence on boththe microbial composi-

tion and diversity of 30 day old *yw seml;NP1>mTOR*$^{RNAi}$.This effect of rapamycin seemed to be independent of its activity on mTORC1.

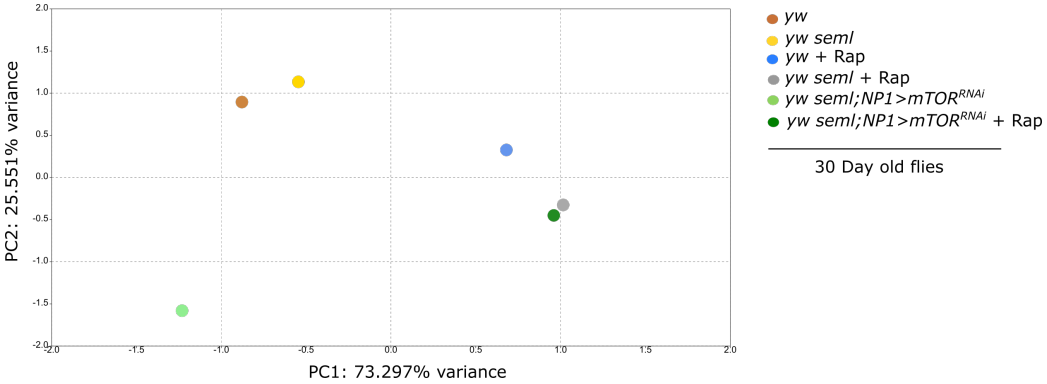



**Figure 3.14: Principal component analysis (PCA) of 30 day old flies treated with rapamycin and/or carrying mTOR$^{RNAi}$.**
The graph represents PCA plot (Beta diversity) of 30 day old fly strains: *yw* (female), *yw seml* (female), *yw* + Rap (female), *yw seml* + Rap (female), *yw seml;NP1>mTOR*$^{RNAi}$ (male), and *yw seml;NP1>mTOR*$^{RNAi}$ + Rap (male). (n=40 guts/strain).

Differences in the bacterial composition between ages and treatments indicated that rapamycin effects the composition and diversity of the gut microbiota in both 5 and 30 day old female *yw* and *yw seml* flies. NGS data and alpha diversity measurements showed that there was no major shift in the microbial composition and diversity of *yw* flies from day 5 to day 30 in both rapamycin treated (*yw* + Rap day 5: Simpson 1-D = 0.4785, Shannon H = 1.107; *yw* + Rap day 30: Simpson 1-D = 0.4278, Shannon H = 0.8452) and untreated (*yw* day 5: Simpson 1-D = 0.7004, Shannon H = 1.673; *yw* day 30: Simpson 1-D = 0.7086, Shannon H = 1.627) conditions **(Figure 3.11 A,B)**. Beta diversity analysis as shown in **Figure 3.15** also suggested a similarity between 5 and 30 day old *yw*, yw+ Rap flies. However, the age dependent

increase in diversity of *yw seml* flies was reversed upon rapamycin treatment **(Figure 3.11 A,B)**. Interestingly, beta diversity analysis (PCA plot) revealed that the dissimilarity between 5 and 30 day old female *yw seml* flies was lost upon treatment with rapamycin **(Figure 3.15)**. Genetic knockdown of mTOR in *seml* male flies showed an age dependent increase in diversity **(Figure 3.11 A,B)**. This was further confirmed by PCA plots, which placed 5 and 30 day old male *yw seml;NP1>mTOR$^{RNAi}$* flies far apart from each other suggesting the role of constitutive loss of mTOR on the composition of the gut microbiota with age **(Figure 3.15)**. Interestingly, 5 day old *yw seml* clustered closely with *yw seml;NP1>mTOR$^{RNAi}$* indicating a similarity in the bacterial composition **(Figure 3.15)**. This suggested that the loss of mTOR does not dictate the diversity of the gut microbiota in young *seml* flies.

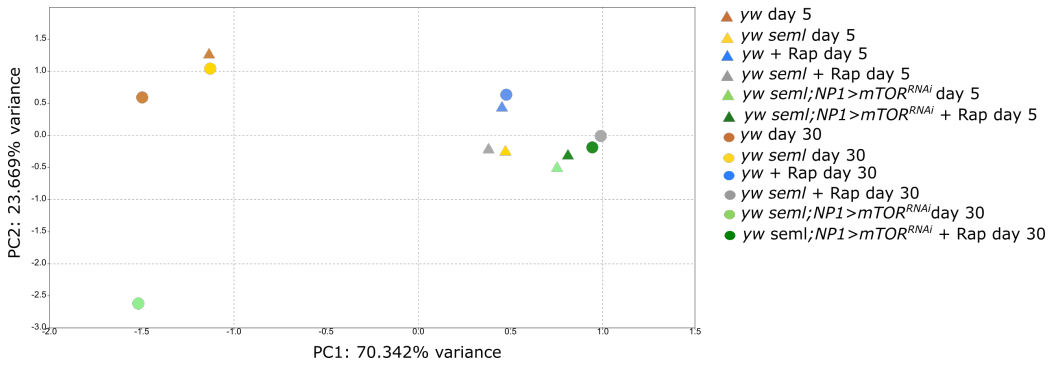



**Figure 3.15: Principal component analysis (PCA) of 5 and 30 day old *yw* and *yw seml* flies treated with rapamycin and/or carrying mTOR$^{RNAi}$.**
The graph represents PCA plot (Beta diversity) of 5 and 30 day old fly strains: *yw* (female), *yw seml* (female), *yw* + Rap (female), *yw seml* + Rap (female), *yw seml;NP1>mTOR$^{RNAi}$* (male), and *yw seml;NP1>mTOR$^{RNAi}$* + Rap (male). (n=40 guts/strain).

## 3.6 Loss of mTOR activity in the gut restores cultivable microbiota in *seml* flies

After testing the role of rapamycin and knockdown of mTOR on the composition of the gut microbiota of *seml* flies, we wanted to test its influence on the microbial load.

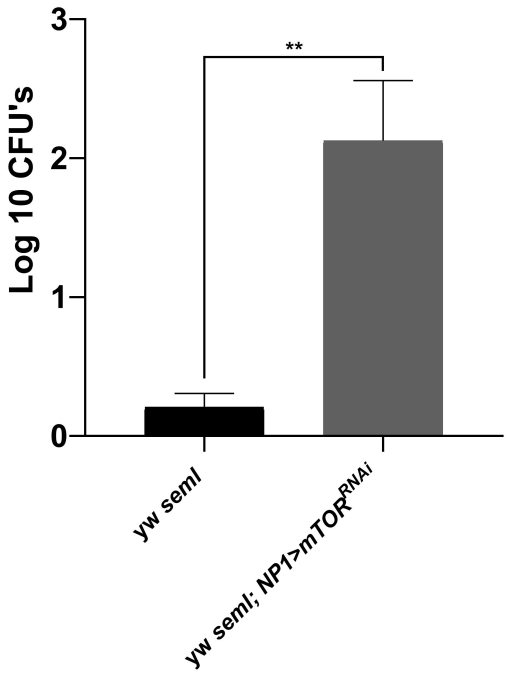



**Figure 3.16: mTOR in the gut is involved in restoration of the cultivable gut microbial load in young *seml* flies.**
The graph represents the cultivable gut microbial load of 5 day old male *yw seml* (n=15), *yw seml;NP1>mTOR$^{RNAi}$* (RNAi of mTOR in enterocyte cells of the gut) flies (n=10). The x axis represents 5 day old fly strains and y axis represents $\log_{10}$ CFU's, (ns = not significant, *p $\leq$ 0.05, **p $\leq$ 0.01, ***p $\leq$ 0.001, ****p $\leq$ 0.0001).

To first check the effect of loss of mTOR on the microbial load of young *seml* flies, we silenced mTOR in the enterocyte cells of *yw seml* flies using the

UAS-GAL4 system and plated them to analyze their microbial load.

As illustrated in **Figure 3.16**, silencing mTOR in enterocyte cells of 5 day old male *seml* mutant flies (n=10) resulted in an 10-fold increase in the cultivable microbial load (student's t-test p-value = 0.004) as compared to *yw seml* flies (n=15). Together with 16S sequencing results as seen in the previous section **(Figure 3.10, 3.11, and 3.12)**, these results indicate that mTOR determines the density but not the diversity of the gut microbiota of young *seml* flies.

Interestingly, a similar observation of restoration of the cultivable gut microbial load was previously seen in the lab when the mTORC1 activity of female *seml* flies was inhibited by rapamycin **(Figure 3.17)**. However, this restoration was observed in 20 day old *seml* flies, which is closer to our 30 day time point. Together these results indicate that rapamycin restores cultivable gut bacteria along with an influence on the diversity of middle aged *seml* flies **(as shown in Figure 3.11, 3.13, and 3.17)**. Nevertheless, the cultivable microbial load of 5 day old *seml* flies treated with rapamycin needs to be tested to confirm results obtained in **Figure 3.16**. Furthermore, the shift in the microbial composition of 30 day old *yw*, *yw seml* and *yw seml;NP1>*$mTOR^{RNAi}$ upon rapamycin treatment (as observed in **(Figure 3.13**) needs to be analyzed for a change in their cultivable microbial load in future studies.

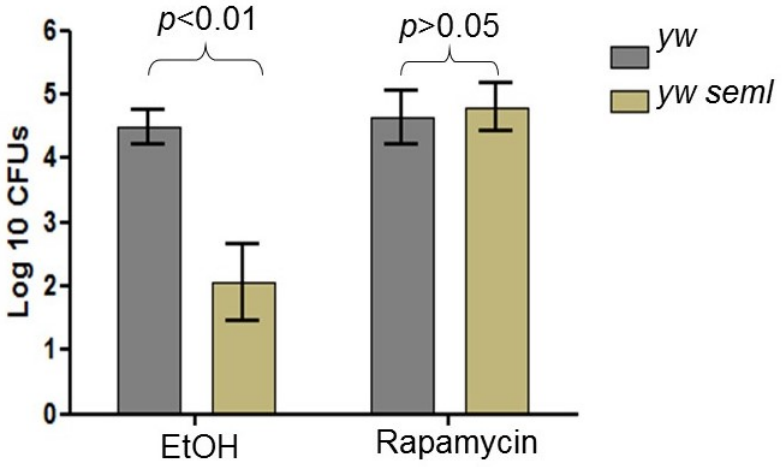



**Figure 3.17: Rapamycin restores the cultivable microbial load in *seml* flies** The graph represents the cultivable gut microbial load of 20 day old female *yw*, *yw seml* flies treated with 200$\mu$M rapamycin and ethanol (vehicle control). The x axis represents fly strains and treatments, and y axis represents $\log_{10}$ CFU's. n= 10-15, (ns = not significant, *p $\leq$ 0.05, **p $\leq$ 0.01, ***p $\leq$ 0.001, ****p $\leq$ 0.0001). Figure taken from Atilano *et al.,* (2018) [120]

## 3.7 Loss of PGRP-SA and DIF alters 4E-BP mRNA levels in young flies

Reduction of the cultivable gut microbiota in *yw seml* and *yw dif*[1] mutant flies as seen in sections 3.1 and 3.3 point towards a metabolic shift of the gut. As previously described, studies have demonstrated that *Drosophila* homologue of mammalian 4E-BP consists of NF-$\kappa$B binding sites in its promoter region, which can be activated by infections that trigger the Toll signalling pathway [99]. Moreover, the role of 4E-BP in regulating protein translation [81] and fat levels [88], made us speculate its role in the cross-talk between immunity and metabolism. We thus wanted to first test if the loss of Toll

signalling pathway components: PGRP-SA and DIF affected the levels of 4E-BP in the *Drosophila* gut.

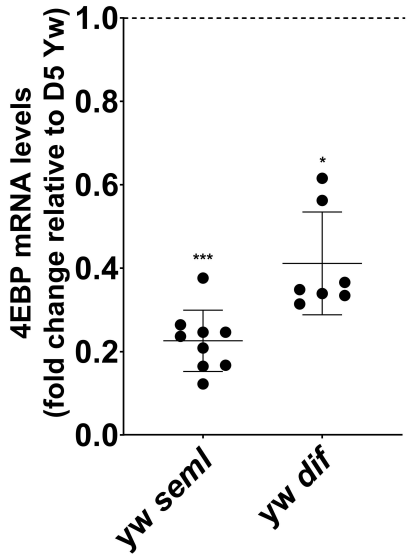



**Figure 3.18: PGRP-SA and DIF influences 4EBP levels in the *Drosophila* gut.** RT-qPCR analysis of 4E-BP expression in the guts of 5 day old female *yw seml* and *yw dif*$^{1}$ flies relative to their genetic background (*yw*) (n=10 guts/strain). The x axis represents different fly strains and the y axis represents relative fold change calculated by $\Delta\Delta C_T$ method. n=3 biological repeats, (ns = not significant, *p $\leq$ 0.05, **p $\leq$ 0.01, ***p $\leq$ 0.001, ****p $\leq$ 0.0001).

qPCR analysis showed a 4-fold decrease of 4E-BP in female *seml* flies (student's t-test p-value = 0.0002) and a 2-fold decrease in female *dif*$^{1}$ flies (student's t-test p-value = 0.0108) as compared to their genetic background (*yw* flies). (n=10 guts/strain) **(Figure 3.18)**. This suggested that the Toll signalling pathway exerts control in the transcription of 4E-BP.

## 3.8 Restoration is associated with 4E-BP mRNA levels

Apart from being controlled by the host innate immunity, the metabolic function of 4E-BP is also known to be regulated by mTORC1. 4E-BP binds to translation initiation factor elF4E and prevents 5'cap-dependent mRNA translation [81]. Activated mTORC1 phosphorylates 4E-BP and promotes translational protein synthesis [81]. To test the effect of genetic and pharmacological inhibition of mTOR activity on 4E-BP levels of *seml* mutant flies, we performed quantitative PCR.

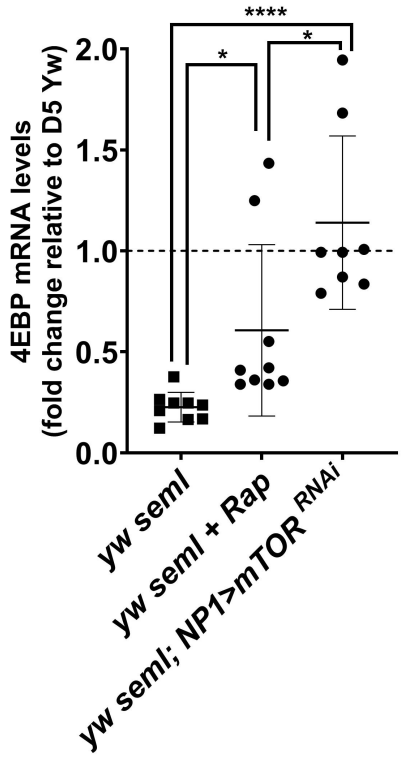



**Figure 3.19: Inhibition of mTOR activity restores 4EBP levels in *seml* mutant *Drosophila* gut.** RT-qPCR analysis of 4E-BP expression in the guts of 5 day old female *yw seml*, female *yw seml* treated with rapamycin and male *yw seml;NP1>mTOR*$^{RNAi}$ flies relative to female *yw* control flies (n=10). The x axis represents different fly strains and the y axis represents relative fold change calculated by $\Delta\Delta C_T$ method. n=3 biological repeats, (ns = not significant, *p $\leq$ 0.05, **p $\leq$ 0.01, ***p $\leq$ 0.001, ****p $\leq$ 0.0001).

Results indicated a 3-fold increase in 4E-BP transcript levels upon rapamycin treatment (female flies) (student's t-test p-value = 0.0174) and a 5-fold increase upon silencing mTOR male flies in the guts of *seml* mutants (student's t-test p-value $\leq$ 0.0001) as compared to 4E-BP levels in the gut of untreated *yw seml* flies **(Figure 3.19)** (n=10 flies/strain). Although an increase in 4E-BP was observed in both cases, loss of mTOR in *seml* mutant flies resulted

in a two fold increase in 4E-BP transcript levels as compared to inhibition of mTORC1 activity by rapamycin (student's t-test p-value = 0.0213). On parallel grounds to the results on the microbial load (as mentioned in section 3.6), a similar restoration pattern was observed in 4E-BP mRNA levels.

We then sought to investigate whether 4E-BP is essential for mediating the restoration of the microbial load by rapamycin in young seml flies which was previously seen in **Figure 3.17**. To do so, we tested the microbial load of male *yw seml;NP1>4E-BP$^{RNAi}$* flies treated rapamycin (n=5) as compared to their untreated counterpart (n=15). Rapamycin treatment had no significant effect on the microbial load (student's t-test p-value = 0.9642) **(Figure 3.20)**, which suggested that rapamycin restores the microbial density in *yw seml* flies through 4E-BP.

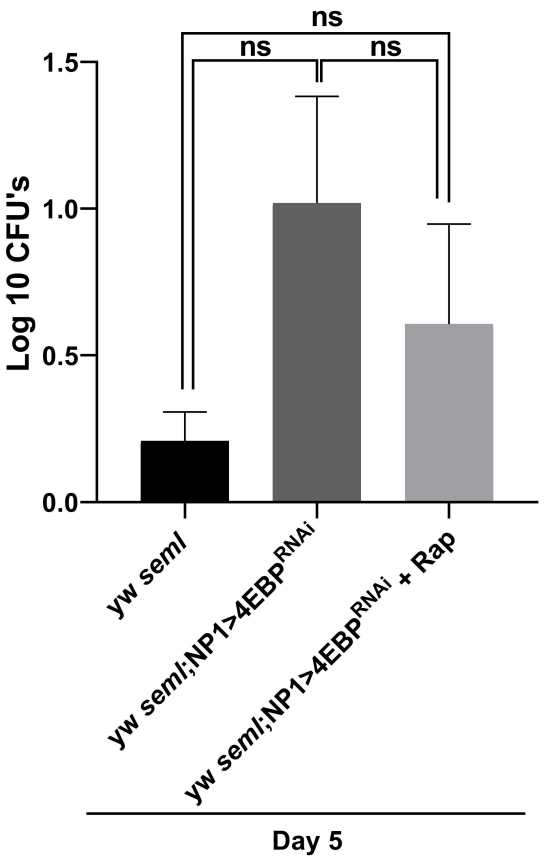



**Figure 3.20: 4E-BP mediates rapamycin induced restoration of cultivable microbial load in *yw seml* flies.** The graph represents the cultivable gut microbial load of 5 day old *yw seml* (male) (n=15), *yw seml;NP1>4E-BP$^{RNAi}$* (male) (n=15) and *yw seml;NP1>4E-BP$^{RNAi}$* + Rap (male) (n=5). The x axis represents different fly strains of different ages, and y axis represents $\log_{10}$ CFU's, (ns = not significant, *p $\leq$ 0.05, **p $\leq$ 0.01, ***p $\leq$ 0.001, ****p $\leq$ 0.0001).

## 3.9 Toll associated NF-$\kappa$B DIF mutants have a reduced lifespan.

To further test the effect of loss of Toll associated NF-$\kappa$B transcription factor DIF, we performed lifespan analysis of *yw dif*$^{1}$ mutants and compared them to their genetic background *yw* flies.

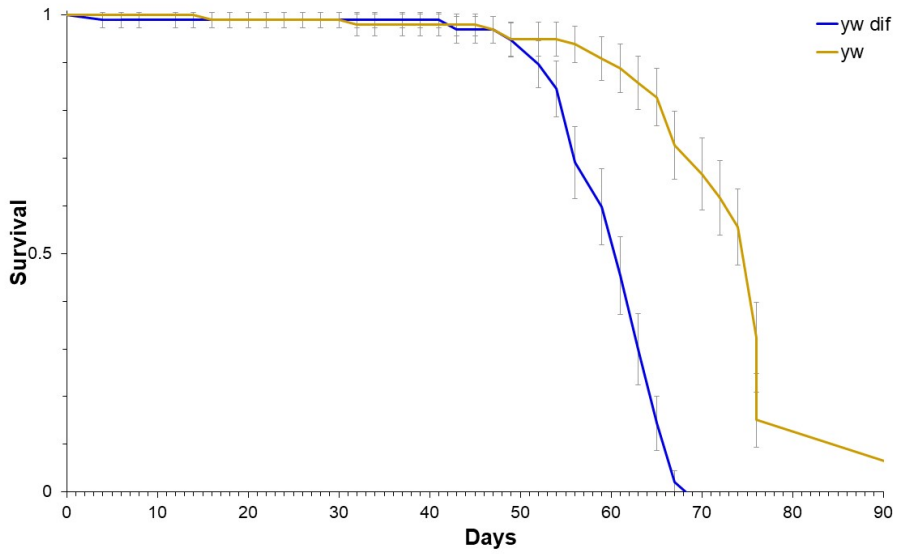



**Figure 3.21: Loss of DIF in *yw dif*$^{1}$ mutant flies reduces its lifespan.**
The graph represents lifespan of *yw* and *yw dif*$^{1}$ female flies. The x axis represents days and y axis represents survival. n=120, (ns = not significant, *p $\leq$ 0.05, **p $\leq$ 0.01, ***p $\leq$ 0.001, ****p $\leq$ 0.0001).

Lifespan curves from this study showed that *yw dif*$^{1}$ female flies (n=120) had a median lifespan of 60 days as compared to 75 days of their genetic background **(Figure 3.21)**. The differences in the survival of *yw* and *yw dif* population of flies was statistically analyzed by performing Log-rank test. This statistical method examines the null hypothesis that at any time

point, no difference is observed between two populations (probability of survival/death) [110]. Log-rank test suggested that the lifespan of *yw dif*$^{1}$ flies significantly differed from their *yw* background control (Chi-squared value for *yw dif*$^{1}$ vs *yw* = 0.034 and log-rank test p-value<0.0001). Shorter lifespan of *dif*$^{1}$ mutant flies indicated the importance of NF-$\kappa$B DIF in the survival of *Drosophila*.

# 4 Discussion

## 4.1 The *Drosophila* Toll signalling pathway interacts with the intestinal microbiota via the peptidoglycan recognition protein PGRP-SA

Tolerance to commensal gut bacteria is mediated by many negative regulators of the IMD pathway in the gut such as Caudal (Inhibits NF-$\kappa$B Relish) [54], Pirk (Disrupts interaction of PGRP-LC/LE with adaptor protein IMD) [53, 121, 122], and PGRP-SC (PGRP family protein, which degrades and reduces levels of PGN) [123]. Recent studies conducted on the PGN recognition protein PGRP-LB have suggested that its extracellular secreted isoform (PGRP-LB$^{PC}$) prevents commensal bacterial PGN from activating the IMD pathway of the fat body [100]. This results in the negative regulation of systemic immune response of the host to the gut bacteria [100]. In this project, we look into the role of Toll signalling pathway in mediating gut microbial homeostasis.

In order to understand how commensal bacteria interact with the Toll signalling pathway in the gut, we studied the extracellular PGN recognition protein PGRP-SA. PGRP-SA along with GNBP1 recognizes Lys-type PGN of Gram positive bacteria outside the cell and initiates the activation of Toll signalling pathway via the transmembrane Toll receptor protein [124]. This in-turn leads to the transcription of AMPs by the NF-$\kappa$B DIF [125]. Our

results indicated that the functional loss of PGRP-SA in young *seml* flies resulted in a reduction of the cultivable microbial load of the gut **(Figure 3.1)**. This was the first indication that PGRP-SA could play a role in presenting the gut microbiota in young flies. A reduction in the cultivable microbial load of the gut was also observed upon loss of GNBP1 in young flies **(Figure 3.4)**. In contrast to this, 30 day old $GNBP1^{osi}$ mutant flies showed a significant increase in the microbial load as compared to its genetic background. Together, these results confirmed that both extracellular PGRP-SA and GNBP1 recognition proteins shared a relationship with the commensal gut bacteria in young flies.

On similar grounds, establishment of a commensal microbial community was described to be mediated by the antibody Immunoglobulin A (IgA) in the human gut [126]. IgA is commonly secreted into the mucosal layer of the gut in the form of sIgA (secretory IgA's). These antibodies play a complex role in mediating commensal bacterial homeostasis together with pathogen clearance [127]. The sIgA forms a protective coating around the commensal bacteria, predominantly via Fab (fragment antigen-binding) dependent interactions [128]. This coating assists in the formation of bio-films, which helps in the steady colonization of endogenous gut microbiota in the intestinal lumen [127]. The role of secretory IgA in establishing a protective environment to the commensal bacteria makes us hypothesize a similar function for PGRP-SA in the *Drosophila* gut.

PGN recognition proteins (PGRPs) are usually expressed in immunocompetent tissues such as fat bodies, haemocytes and the gut [129]. Due to the close vicinity of the commensal bacteria and the gut epithelia, we wanted to check if the PGRP-SA produced in the gut interacts with the indigenous bacteria. Using enterocyte cell specific (gut epithelium) knockdown of PGRP-SA, we showed that PGRP-SA produced in the gut is required for the maintenance of the commensal microbial load **(Figure 3.3)**. Other sources of PGRP-SA will be tested by producing site specific knockdowns of PGRP-SA in the fat body and haemocytes, and analyzing their effects on the commensal bacteria.

Reduction in the microbial load upon functional loss of PGRP-SA made us speculate the involvement of other downstream components of the Toll signalling pathway. To this end, we tested the influence of the Toll signalling pathway associated NF-$\kappa$B DIF in regulating the commensal microbial load of flies. Using ($dif^1$) flies, we showed that DIF is important for maintaining the commensal microbial load in young flies **(Figure 3.5)**. This could be explained by a reduction in the production of PGRP-SA via a positive feedback loop in the Toll signalling pathway [130, 131].

## 4.2 PGRP-SA promotes Lactobacillaceae retention in young *Drosophila* gut

Comparative analysis of 16S sequences obtained from the gut microbiota of 5 day old *seml* flies revealed that PGRP-SA associates with the Lactobacillaceae family in the gut. However, this association appears to decrease as the fly ages **(Figure 3.7)**. This age dependent variation of the abundance of Lactobacillaceae in *seml* flies is associated with an increase in diversity pattern which remains almost constant in *yw* flies **(Figure 3.8)**. Loss of cultivable microbial load in young *seml* flies can be attributed to the reduction of Lactobacillaceae. However, with age, the recovery of Lactobacillaceae could be dictated by food and diet, which replaces the microbiota shaped by familial transmission. Together, we speculate that PGRP-SA interacts with the dominant Lactobacillaceae species (mainly Gram-positive) and promote its colonization in the mucosal layer of young flies.

## 4.3 mTOR pathway regulates microbial composition in normal and immune compromised flies

mTOR is a major player in modulating the metabolic status of the host [79]. It's activity is controlled by various upstream cues such as amino acid [77], insulin [70], and energy status [132] of the cell, levels of which are diet dependent. Our results indicated that genetic ($\text{mTOR}^{RNAi}$) or pharmacological (rapamycin) inhibition of mTOR activity in immune compromised

*seml* flies of ages 5 and 20 day old respectively, restored its cultivable gut microbiota **(Figure 3.16 and 3.17)**. Deep sequencing analysis showed that silencing mTOR in 5 day old *seml* flies (*yw seml;NP1>mTOR*$^{RNAi}$) did not considerably affect the composition and diversity of its gut microbiota as compared to 5 day old *seml* flies. This suggests that restoration of the microbial load is a consequence of a shift in the microbial density of the already existing microbiota rather than an increase in diversity. A similar pattern of the change in gut microbial composition was seen when young *seml* flies were fed with rapamycin food **(Figure 3.10)**. However, we need to test if rapamycin treatment restores the cultivable microbial load of young *seml* flies. This would help in confirming the importance of mTOR activity in determining the microbial density in young immune compromised *seml* flies as seen in mTOR knockdown studies.

In contrast to the aforementioned results, 30 day old *seml* flies had a distinct composition of the indigenous microbiota upon inhibition of mTOR activity, which was different from 30 day old *seml* flies. Moreover, our results showed a substantial shift in the microbial diversity, which was brought upon in 30 day old *seml* flies by genetically (mTOR$^{RNAi}$) or pharmacologically (rapamycin) inhibiting the mTOR activity , as compared to 30 day old untreated *seml* flies **(Figure 3.13)**. Interestingly, our results also showed that feeding rapamycin to 30 day old *yw seml*, and *yw seml;NP1>mTOR*$^{RNAi}$ resulted in the development of a microbial composition similar to that of 30 day old

*yw* flies fed with rapamycin as shown in the PCA plot **(Figure 3.15)**. 16S analysis of middle age flies, fed with rapamycin in our study is in line with other studies, which also describes the effects of rapamycin on the microbial composition of aged flies and mice [97, 133].

Together, both 5 and 30 day old 16S results suggest that rapamycin has a differential effect on the microbial composition of immune compromised *seml* flies, which is dependent on its age and time of treatment. Moreover, rapamycin reduces the abundance of Lactobacillaceae in both ages, regardless of the immune status of the fly **(Figure 3.10 and 3.13)**. This antagonistic trend between rapamycin and Lactobacillaceae family was also shown in different studies conducted on mice and flies [95, 134].

## 4.4 Drosophila 4E-BP mediates cross-talk between host-metabolism and immunity with gut microbiota

Our observations on the effect of inhibition of the mTOR activity motivated us to study the role of its downstream target 4E-BP in serving as a mediator in the host-microbiome cross-talk. Activated mTORC1 promotes protein synthesis by inhibiting the activity of the translation regulating factor 4E-BP [81]. Rapamycin induced inhibition of mTORC1 restores 4E-BP levels, which promotes accumulation of fat [88] and regulation of amino acid pool [135] in wild type *Drosophila*.

Our results indicate that knockdown of 4E-BP in the gut epithelia of *Drosophila* resulted in a significant loss of cultivable microbial load **(Supplementary Figure 5.5)**. This could probably be due to a reduction in the levels of accumulated fat and a variation in the amino acid levels, both of which may serve as nutrient source for commensal microbes. Reduction of 4E-BP mRNA levels in young *seml* mutant flies **(Figure 3.18)** correlated with the loss of microbial load in 4E-BP knockdown flies, confirming that Toll signalling pathway influences 4E-BP levels, which was also observed by Bernal *et al.,* (2000) [99]. Moreover, we showed that genetic ($mTOR^{RNAi}$) or pharmacological (rapamycin) inhibition of mTOR activity in *seml* flies resulted in an increase in 4E-BP levels **(Figure 3.19)**, which shared a similar pattern with the cultivable microbiota studies **(Figure 3.16 and 3.17)**. Finally, our study on the cultivable microbial load of *yw seml;NP1>4E-BP*$^{RNAi}$ treated with rapamycin **(Figure 3.20)** indicate that 4E-BP is essential for the function of rapamycin in the restoration of microbial load. Further studies are needed to characterize the importance of regulation of metabolites by 4E-BP in maintaining gut microbiota homeostasis.

## 4.5 Conclusion

In conclusion, extracellular PGRP-SA is essential for maintaining commensal microbial homeostasis in young flies, which may share functional homology with sIgA in humans. Furthermore, 4E-BP plays a key role in linking the innate immune Toll signalling pathway and metabolic mTOR pathway. More-

over, cross-talk between Toll and mTOR pathway determines the microbial load and composition through alteration of nutrient levels via 4E-BP in the gut **(Figure 4.1)**. Impairment of this balance, either by aberrations in the Toll signalling pathway or mTOR pathway can result in an imbalance of 4E-BP levels, thereby resulting in dysbiosis. Interestingly, this mechanism of gut microbial homeostasis is only observed in young flies and experiments have to be performed to understand the age dependent shift in the complex relationship between immunity, metabolism and gut microbiota in *Drosophila*.

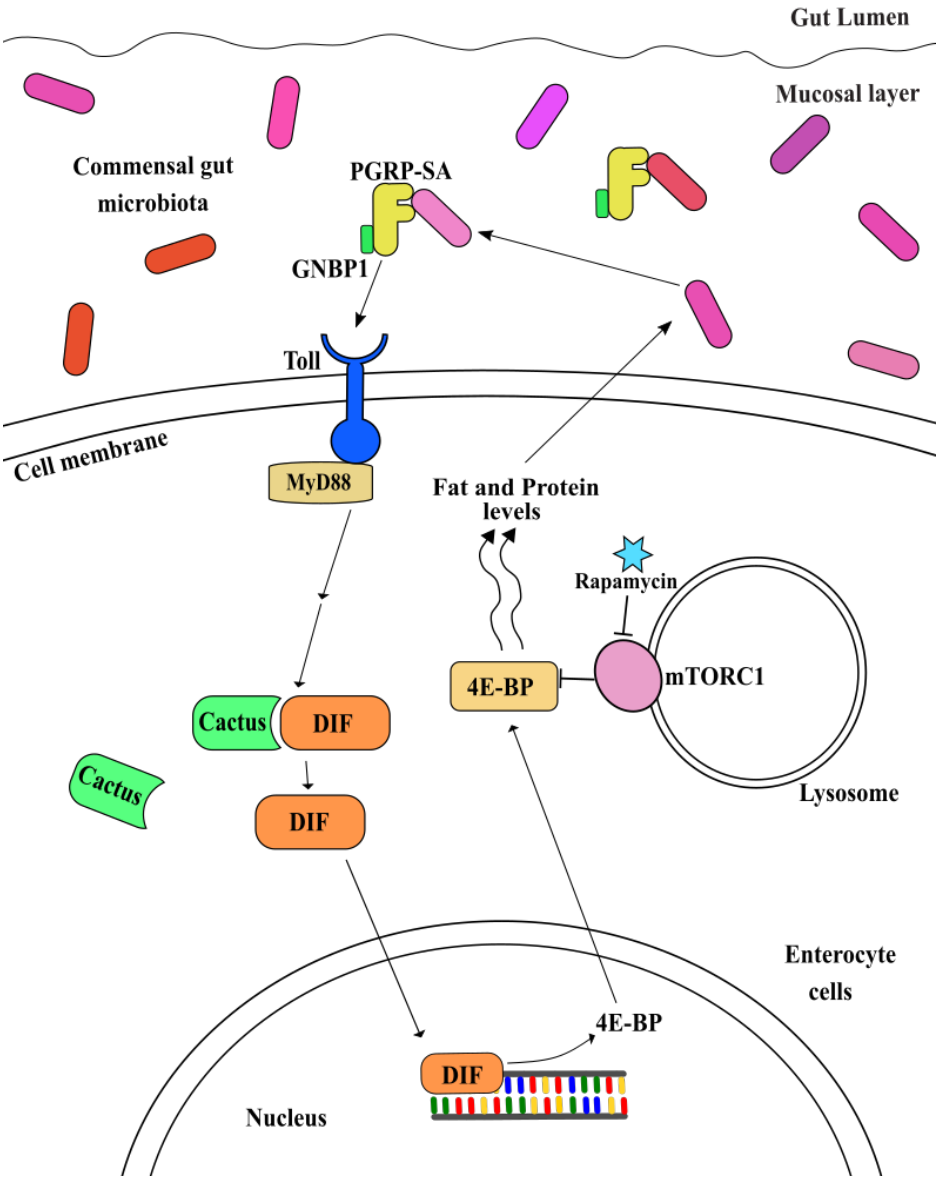



**Figure 4.1: Innate immune Toll and metabolic mTOR pathways interact to shape the gut microbiota of *Drosophila melanogaster***

## 4.6 Future directions

This project has brought us on the path of understanding how the immune and metabolic system of the host balance with each other to shape and maintain gut microbial homeostasis. Through this study, we highlighted the important role of PGRP-SA in preserving the gut microbiota (especially bacteria belonging to the family Lactobacillaceae). We also showed that 4E-BP could potentially mediate the balance between host immunity and metabolism, and maintain gut microbial homeostasis. However, many more experiments have to be performed to confirm the above findings, and answer other major questions such as the ones enlisted below:

**Does PGRP-SA preserve Lactobacillaceae in the gut of young flies?**

As reported in **Figure 3.7**, mutation of the *pgrp-sa* gene in young *seml* flies resulted in a substantial loss of Lactobacillaceae. Therefore, it would be interesting to check if PGRP-SA retains/protects Lactobacillaceae in the gut. This can be tested by feeding germ free *seml* flies with sterile food, enriched with fluorescent Lactobacillaceae and tracking them in the gut. This experiment can also performed to test if PGRP-SA retains Lactobacillaceae in both young and middle age flies.

**Are Lactobacillaceae susceptible to rapamycin treatment?**

NGS data showed that treating both 5 and 30 day old flies with a transient dose of rapamycin resulted in a loss of Lactobacillaceae **(Figure 3.10 and**

**3.13)**. This raises questions on whether this loss is dependent on the inhibition of mTORC1 and/or its antibiotic activity. We can examine the possible antibiotic activity of rapamycin by testing its toxicity to the cultivable gut microbiota by plating bacterial colonies residing in the *Drosophila* gut on MRS plates supplemented with rapamycin. Furthermore, mono-associating and imaging fluorescent Lactobacillaceae in rapamycin treated flies can also provide insights into the effect of rapamycin on Lactobacillaceae.

**Does 4E-BP maintain gut microbial homeostasis by regulating fat levels?**

As previously mentioned, *Teleman et al.,* (2005) showed that increasing the activity of 4E-BP by rapamycin treatment resulted in an increase in the levels of accumulated fat [88]. However, mutants of 4E-BP did not show the same phenotype upon rapamycin treatment [88]. A similar trend of the cultivable gut microbial load was observed when *yw seml;NP1>4E-BP*$^{RNAi}$ were treated rapamycin. To assess the relationship between fat levels and microbial load, We can analyze the fat levels of all the mutant flies that are described in this project, and compare them with the existing microbiota results.

**Is sex more important than the genetic factors of the host in shaping the microbiota?**

A limitation in this study was the possible sex based differences in the gut microbiota, which must be addressed in the future. This limitation in the study is due to *pgrp-sa* residing on the X chromosome. Michel *et al.,* (2001) first described *seml* mutants as flies having a point mutation in the first (x) chromosome ($x^{seml}$) [101]. In order to preserve this mutation in the progeny, crosses were set up, in which homozygous *seml* females ($x^{seml}x^{seml}$) were crossed with wild type GAL4 driver males (xy) to yield heterozygous *seml* females ($x^{seml}x$) and hemizygous males ($x^{seml}y$). Hemizygous males exhibited *seml* mutation, and hence were selected for studies involving *ywseml*,NP1>$mTOR^{RNAi}$ or *ywseml*,NP1>$4E\text{-}BP^{RNAi}$ double mutants. Heterozygous females on the other hand, expressed normal PGRP-SA, and thus were not used in the study. This raised the question of sex based comparisons with regard to the bacterial composition between different fly strains. We can address this issue by preparing GAL4 drivers with x linked *seml* mutation for the crosses. Crossing these *seml*;GAL4 drivers with *seml* UAS lines will result in homozygous progeny females ($x^{seml}x^{seml}$), which can be used to study and compare the microbial composition of the gut. This would help in eliminating any sex based differences in the study.

**Does genetic background effect the bacterial composition?**

Regardless of a significant difference in the microbial load of DGRP *25174* flies as compared to *yw* flies (student's t-test p-value = 0.0019) **(Supplementary Figure 5.6)**, considerable loss of the microbial load of young *seml* and *dif* mutants (in both *25174*, *yw* genetic backgrounds) indicated that the genetic background does not majorly effect the bacterial load of immune-mutant flies **(Figure 3.2 and 3.6)**. However, we need to perform 16S sequencing, rapamycin studies and lifespan analysis of these mutants in the *25174* background, and compare them with *yw* mutant flies to check the relation of the gut microbiota on the genetic background of the fly.

With the remaining time after submission, and with the help of the next master's student, we will aim to answer the above enlisted questions. The larger objective of this study will not only be to understand the immune and metabolic balance of the host in the context of gut microbiota in healthy flies, but we will also look into exploring the variations in this balance in dysbiosis and disease models.

# 5 Appendix

## 5.1 Fly food recipe

| **Reagent** | **Amount (mass/vol)** |
|---|---|
| Maize Flour (Brian Drewitt) | 1.8kg |
| Malt Extract (Brian Drewitt) | 1.8kg |
| Molasses (Rayners, Brian Drewitt) | 500g |
| Soya Flour (Brian Drewitt) | 216g |
| Yeast Powder (Brian Drewitt) | 366g |
| Agar (Fisher Scientific, BPE2641-1) | 169g |
| Methyl 4-hydroxybenzoate (Nipagin, Sigma-Aldrich W271004) | 74g |
| Ethanol (VWR) | 703ml |
| 95% propionic acid (Sigma-Aldrich P5561), 5% phosphoric acid (Sigma-Aldrich P5811) solution | 140ml |
| Water | 28L |

**Table 5.1:** Composition of conventional fly food used in this project.

## 5.2 De Man, Rogosa and Sharpe (MRS) media composition

| **Reagent** | **Amount (gm/litre)** |
|---|---|
| Peptone | 10g |
| 'Lab-Lemco' powder | 8g |
| Yeast extract | 4g |
| Glucose | 20g |
| Sorbitan mono-oleate | 1ml |
| Dipotassium hydrogen phosphate | 2g |
| Sodium acetate $3H_2O$ | 5g |
| Triammonium citrate | 2g |
| Magnesium sulphate $7H_2O$ | 0.2g |
| Manganese sulphate $4H_2O$ | 0.05g |
| Agar | 10g |
| pH 6.2 $\pm$ 0.2 @ 25°C | |

**Table 5.2:** Composition of de Man, Rogosa and Sharpe (MRS) agar for analyzing the cultivable gut microbial load of flies.

## 5.3 Relative abundance of 5 day old *yw*(R) and *yw seml*(R)

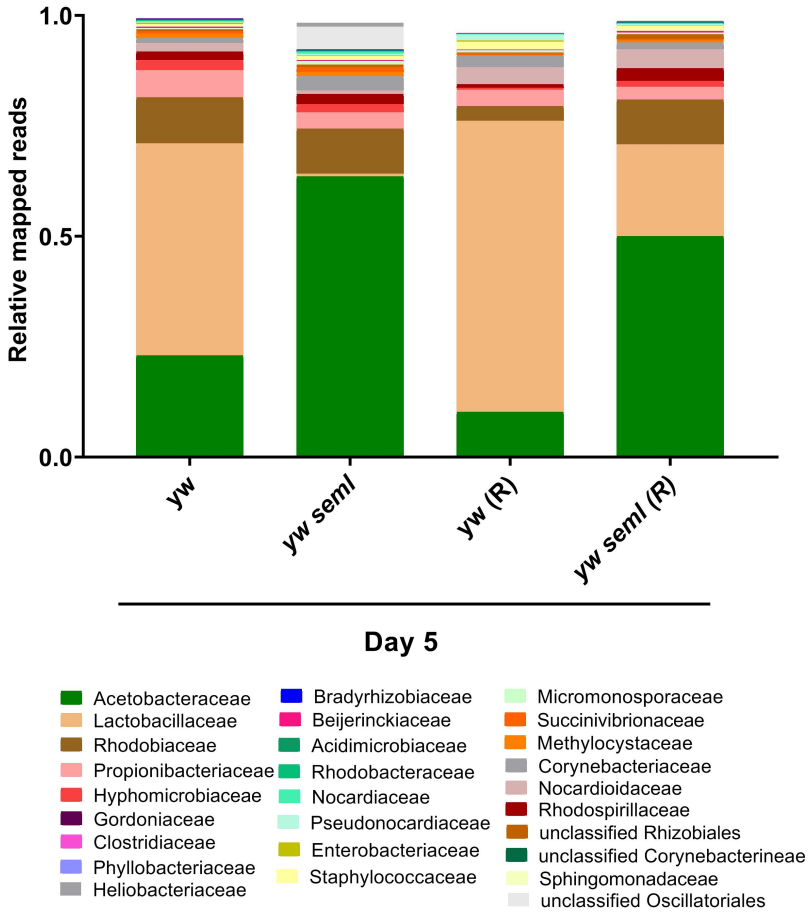



**Figure 5.1: Relative bacterial abundance of biological repeats of 5 day old *yw* and *yw seml* flies**
The graph represents the relative abundance of microbial families observed in the biological repeats of 5 day old *yw*, *yw seml* flies as revealed by 16S next generation sequencing. The x axis represents fly strains, and the y axis represents relative mapped reads. (n=40 guts/strain).

## 5.4 Relative abundance of enterocyte specific mTOR knockdown

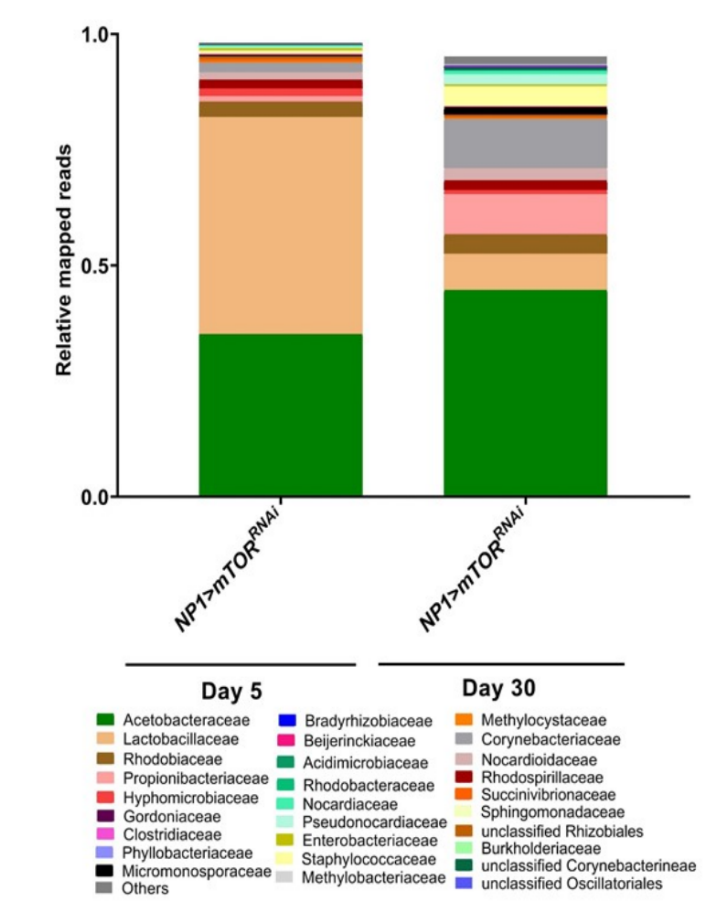



**Figure 5.2: Relative bacterial abundance of enterocyte specific mTOR knockdown flies of different ages.**
The graph represents the relative abundance of microbial families observed in 5 and 30 day old NP1>mTOR$^{RNAi}$ flies as revealed by 16S next generation sequencing. The x axis represents fly strains of different ages, and the y axis represents relative mapped reads. (n=40 guts/strain).

## 5.5 Gut microbial composition of 5 day old metabolic mutant flies

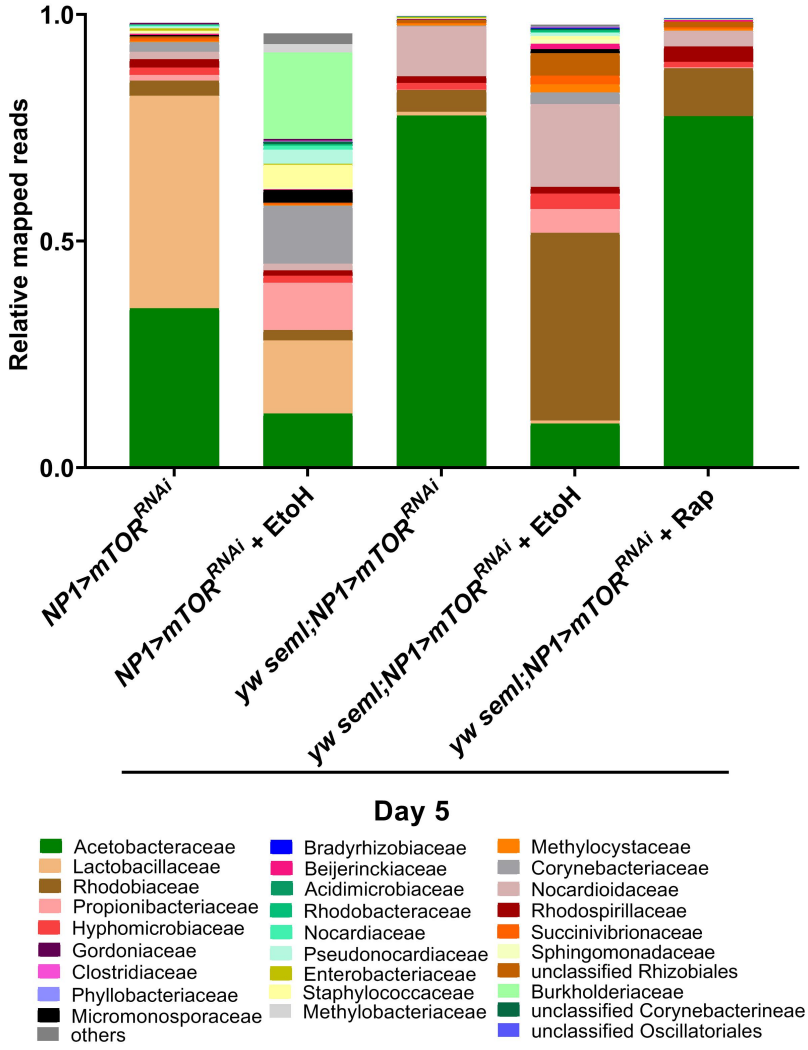



**Figure 5.3: Relative bacterial abundance of 5 day old metabolic mutants.** The graph represents the relative abundance of microbial families observed in 5 day old metabolic mutant flies as revealed by 16S next generation sequencing. The x axis represents different fly strains, and the y axis represents relative mapped reads. (n=40 guts/strain).

## 5.6 Gut microbial composition of 30 day old metabolic mutant flies

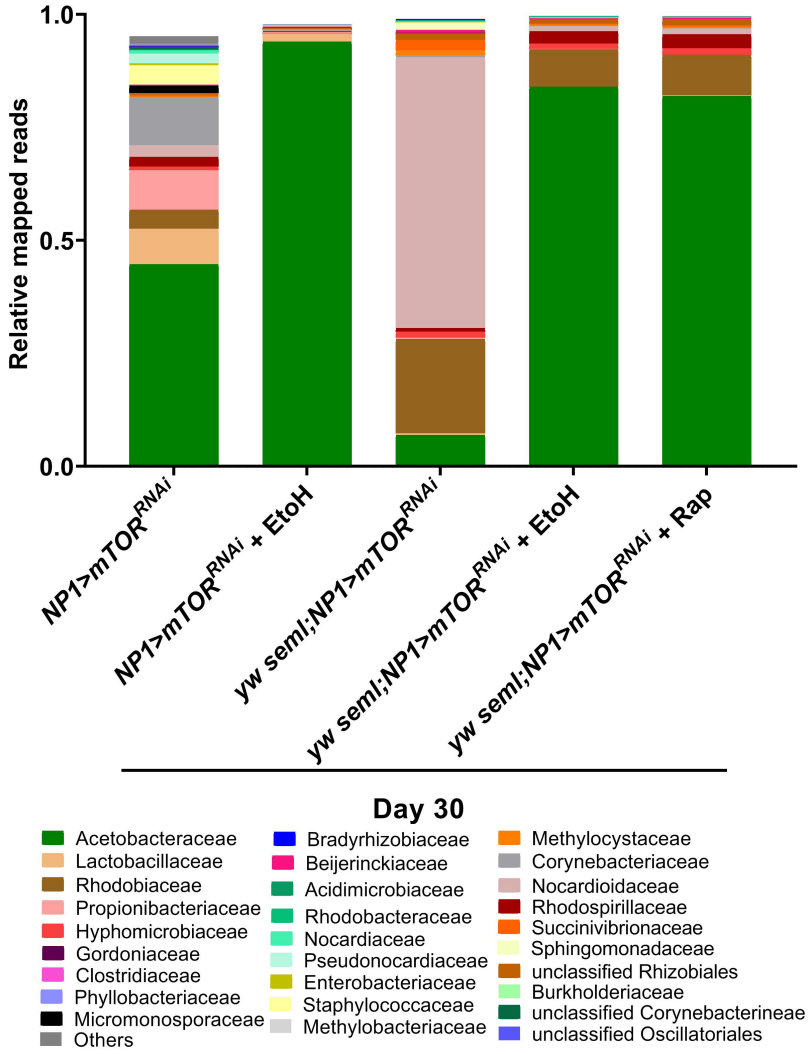



**Figure 5.4: Relative bacterial abundance of 30 day old metabolic mutants.** The graph represents the relative abundance of microbial families observed in 30 day old metabolic mutant flies as revealed by 16S next generation sequencing. The x axis represents different fly strains, and the y axis represents relative mapped reads. (n=40 guts/strain).

## 5.7 Alpha diversity index values

| **Fly strains** | **Simpson 1-D** | **Shanon H** | **$S_{obs}$** |
|---|---|---|---|
| *yw* day 5 | 0.7004 | 1.673 | 116 |
| *yw seml* day 5 | 0.5768 | 1.499 | 149 |
| *yw day* 30 | 0.7086 | 1.627 | 117 |
| *yw seml* day 30 | 0.7465 | 1.864 | 150 |
| *yw* + Rap day 5 | 0.4785 | 1.107 | 118 |
| *yw seml* + Rap day 5 | 0.5878 | 1.37 | 141 |
| *yw seml;NP1>mTOR$^{RNAi}$* day 5 | 0.3825 | 0.9148 | 105 |
| *yw seml;NP1>mTOR$^{RNAi}$* + Rap day 5 | 0.386 | 0.927 | 126 |
| *yw* + Rap day 30 | 0.4278 | 0.8452 | 110 |
| *yw seml* + Rap day 30 | 0.2836 | 0.7219 | 87 |
| *yw seml;NP1>mTOR$^{RNAi}$ day 30* | 0.5917 | 1.386 | 135 |
| yw seml;NP1>mTOR$^{RNAi}$ + Rap day 30 | 0.321 | 0.7853 | 103 |

**Table 5.3:** $S_{obs}$, Simpson (1-D) and Shannon H alpha diversity index values of the microbial composition of different fly strains and treatments observed in this study.

## 5.8 Cultivable gut microbial load of metabolic mutant flies

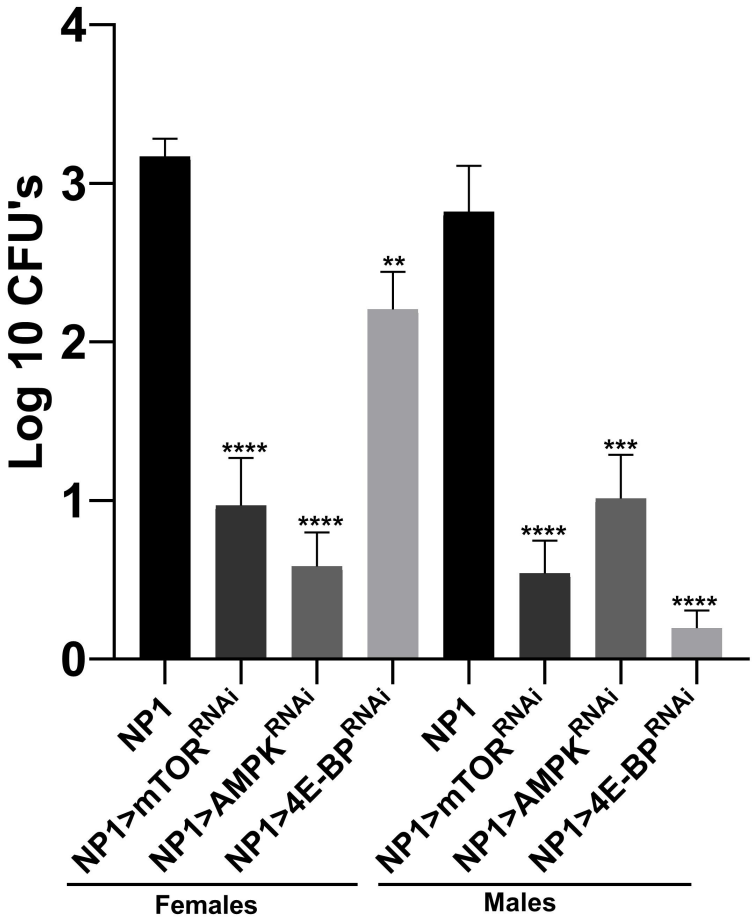



**Figure 5.5: Components of the mTOR pathway (mTOR, AMPK, and 4E-BP) in the gut influences the cultivable microbial load in young flies.**
The graph represents the cultivable gut microbial load of 5 day old enterocyte specific (NP1-GAL4) RNAi's of mTOR, AMPK, and 4E-BP flies of both sexes. The x axis represents fly strains and y axis represents $\log_{10}$ CFU's, n=10-15 (ns = not significant, *p $\leq$ 0.05, **p $\leq$ 0.01, ***p $\leq$ 0.001, ****p $\leq$ 0.0001).

## 5.9 Cultivable gut microbial load of *yw* and *25174* genetic background

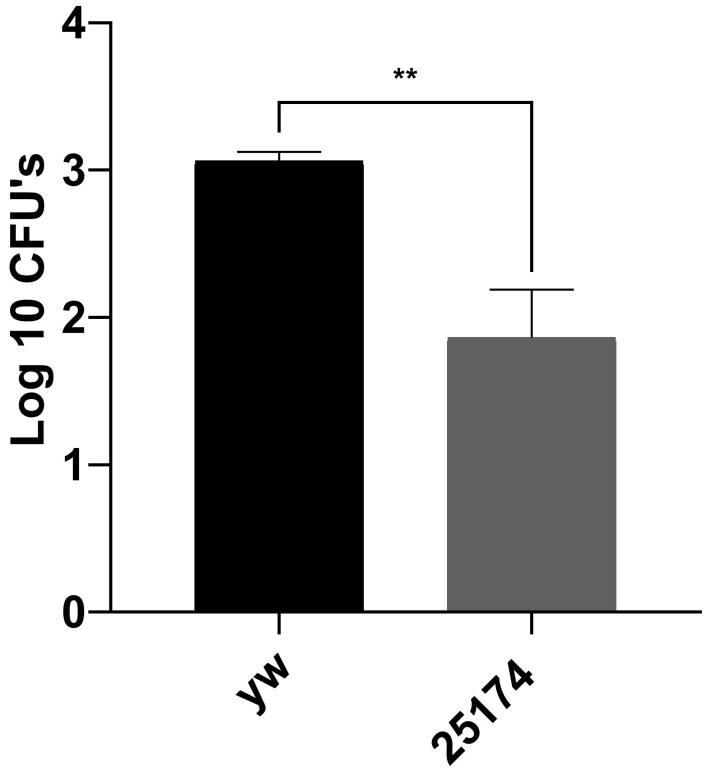



**Figure 5.6: Microbial load of *Drosophila melanogaster* depends on the genetic background (*yw* v/s DGRP *25174*).**
The graph represents the cultivable gut microbial load of 5 day old female *yw* and DGRP *25174* flies. The x axis represents fly strains and y axis represents $\log_{10}$ CFU's, n=10-15 (ns = not significant, *p $\leq$ 0.05, **p $\leq$ 0.01, ***p $\leq$ 0.001, ****p $\leq$ 0.0001).

# References


1. Cani, P. D. Human gut microbiome: hopes, threats and promises. *Gut* **67,** 1716–1725 (2018).

2. Muegge, B. D. *et al.* Diet drives convergence in gut microbiome functions across mammalian phylogeny and within humans. *Science* **332,** 970–974 (2011).

3. Sekirov, I., Russell, S. L., Antunes, L. C. M. & Finlay, B. B. Gut microbiota in health and disease. *Physiological reviews* **90,** 859–904 (2010).

4. Walter, J., Britton, R. A. & Roos, S. Host-microbial symbiosis in the vertebrate gastrointestinal tract and the Lactobacillus reuteri paradigm. *Proceedings of the National Academy of Sciences* **108,** 4645–4652 (2011).

5. Korpela, K. *et al.* Selective maternal seeding and environment shape the human gut microbiome. *Genome research* **28,** 561–568 (2018).

6. Schroeder, B. O. Fight them or feed them: how the intestinal mucus layer manages the gut microbiota. *Gastroenterology report* **7,** 3–12 (2019).

7. Morgan, X. C. *et al.* Dysfunction of the intestinal microbiome in inflammatory bowel disease and treatment. *Genome biology* **13,** R79 (2012).

8. Wirbel, J. *et al.* Meta-analysis of fecal metagenomes reveals global microbial signatures that are specific for colorectal cancer. *Nature medicine* **25,** 679 (2019).

9. Thomas, A. M. *et al.* Metagenomic analysis of colorectal cancer datasets identifies cross-cohort microbial diagnostic signatures and a link with choline degradation. *Nature medicine* **25,** 667 (2019).

10. Tremaroli, V. *et al.* Roux-en-Y gastric bypass and vertical banded gastroplasty induce long-term changes on the human gut microbiome contributing to fat mass regulation. *Cell metabolism* **22,** 228–238 (2015).

11. Ley, R. E., Turnbaugh, P. J., Klein, S. & Gordon, J. I. Microbial ecology: human gut microbes associated with obesity. *nature* **444,** 1022 (2006).

12. Karlsson, F. H. *et al.* Gut metagenome in European women with normal, impaired and diabetic glucose control. *Nature* **498,** 99 (2013).

13. Llopis, M. *et al.* Lactobacillus casei downregulates commensals' inflammatory signals in Crohn's disease mucosa. *Inflammatory bowel diseases* **15,** 275–283 (2008).

14. Qin, J. *et al.* A metagenome-wide association study of gut microbiota in type 2 diabetes. *Nature* **490,** 55 (2012).

15. Kong, C., Gao, R., Yan, X., Huang, L. & Qin, H. Probiotics improve gut microbiota dysbiosis in obese mice fed a high-fat or high-sucrose diet. *Nutrition* **60,** 175–184 (2019).

16. Chen, D., Wu, J., Jin, D., Wang, B. & Cao, H. Fecal microbiota transplantation in cancer management: Current status and perspectives. *International journal of cancer* (2018).

17. Sartor, R. Role of the enteric microflora in the pathogenesis of intestinal inflammation and arthritis. *Alimentary pharmacology & therapeutics* **11,** 17–23 (1997).

18. Bouma, G. & Strober, W. The immunological and genetic basis of inflammatory bowel disease. *Nature reviews immunology* **3,** 521 (2003).

19. Sender, R., Fuchs, S. & Milo, R. Are we really vastly outnumbered? Revisiting the ratio of bacterial to host cells in humans. *Cell* **164,** 337–340 (2016).

20. Gilbert, J. A. *et al.* Current understanding of the human microbiome. *Nature medicine* **24,** 392 (2018).

21. Rinninella, E. *et al.* What is the healthy gut microbiota composition? a changing ecosystem across age, environment, diet, and diseases. *Microorganisms* **7,** 14 (2019).

22. Jandhyala, S. M. *et al.* Role of the normal gut microbiota. *World journal of gastroenterology: WJG* **21,** 8787 (2015).

23. De Filippo, C. *et al.* Impact of diet in shaping gut microbiota revealed by a comparative study in children from Europe and rural Africa. *Proceedings of the National Academy of Sciences* **107,** 14691–14696 (2010).

24. Brooks, A. W., Priya, S., Blekhman, R. & Bordenstein, S. R. Gut microbiota diversity across ethnicities in the United States. *PLoS biology* **16,** e2006842 (2018).

25. Jones, R. B. *et al.* Inter-niche and inter-individual variation in gut microbial community assessment using stool, rectal swab, and mucosal samples. *Scientific reports* **8,** 4139 (2018).

26. Kho, Z. Y. & Lal, S. K. The human gut microbiome–a potential controller of wellness and disease. *Frontiers in microbiology* **9** (2018).

27. Broderick, N. A. & Lemaitre, B. Gut-associated microbes of Drosophila melanogaster. *Gut microbes* **3,** 307–321 (2012).

28. Wong, C. N. A., Ng, P. & Douglas, A. E. Low-diversity bacterial community in the gut of the fruitfly Drosophila melanogaster. *Environmental microbiology* **13,** 1889–1900 (2011).

29. Bakula, M. The persistence of a microbial flora during postembryogenesis of Drosophila melanogaster. *Journal of invertebrate pathology* **14,** 365–374 (1969).

30. Ren, C., Webster, P., Finkel, S. E. & Tower, J. Increased internal and external bacterial load during Drosophila aging without life-span trade-off. *Cell metabolism* **6,** 144–152 (2007).

31. Kounatidis, I. & Ligoxygakis, P. Drosophila as a model system to unravel the layers of innate immunity to infection. *Open biology* **2,** 120075 (2012).

32. Chandler, J. A., Lang, J. M., Bhatnagar, S., Eisen, J. A. & Kopp, A. Bacterial communities of diverse Drosophila species: ecological context of a host–microbe model system. *PLoS genetics* **7,** e1002272 (2011).

33. Corby-Harris, V. *et al.* Geographical distribution and diversity of bacteria associated with natural populations of Drosophila melanogaster. *Appl. Environ. Microbiol.* **73,** 3470–3479 (2007).

34. Mistry, R., Kounatidis, I. & Ligoxygakis, P. Interaction between familial transmission and a constitutively active immune system shapes gut microbiota in Drosophila melanogaster. *Genetics* **206,** 889–904 (2017).

35. Kau, A. L., Ahern, P. P., Griffin, N. W., Goodman, A. L. & Gordon, J. I. Human nutrition, the gut microbiome and the immune system. *Nature* **474,** 327 (2011).

36. Bull, M. J. & Plummer, N. T. Part 1: The human gut microbiome in health and disease. *Integrative Medicine: A Clinician's Journal* **13,** 17 (2014).

37. Wong, A. C.-N., Dobson, A. J. & Douglas, A. E. Gut microbiota dictates the metabolic response of Drosophila to diet. *Journal of Experimental Biology* **217,** 1894–1901 (2014).

38. Kostic, A. D., Howitt, M. R. & Garrett, W. S. Exploring host–microbiota interactions in animal models and humans. *Genes & development* **27,** 701–718 (2013).

39. Wong, A. C., Vanhove, A. S. & Watnick, P. I. The interplay between intestinal bacteria and host metabolism in health and disease: lessons from Drosophila melanogaster. *Disease models & mechanisms* **9,** 271–281 (2016).

40. Sansonetti, P. J. & Medzhitov, R. Learning tolerance while fighting ignorance. *Cell* **138,** 416–420 (2009).

41. Govind, S. Innate immunity in Drosophila: Pathogens and pathways. *Insect science* **15,** 29–43 (2008).

42. Myllymäki, H., Valanne, S. & Rämet, M. The Drosophila imd signaling pathway. *The Journal of Immunology* **192,** 3455–3462 (2014).

43. Valanne, S., Wang, J.-H. & Rämet, M. The Drosophila toll signaling pathway. *The Journal of Immunology* **186,** 649–656 (2011).

44. Wang, L. *et al.* Sensing of Gram-positive bacteria in Drosophila: GNBP1 is needed to process and present peptidoglycan to PGRP-SA. *The EMBO journal* **25,** 5005–5014 (2006).

45. El Chamy, L., Leclerc, V., Caldelari, I. & Reichhart, J.-M. Sensing of'danger signals' and pathogen-associated molecular patterns defines binary signaling pathways' upstream'of Toll. *Nature immunology* **9,** 1165 (2008).

46. Jang, I.-H. *et al.* A Spätzle-processing enzyme required for toll signaling activation in Drosophila innate immunity. *Developmental cell* **10,** 45–55 (2006).

47. Horng, T. & Medzhitov, R. Drosophila MyD88 is an adapter in the Toll signaling pathway. *Proceedings of the National Academy of Sciences* **98,** 12654–12658 (2001).

48. Towb, P., Bergmann, A. & Wasserman, S. A. The protein kinase Pelle mediates feedback regulation in the Drosophila Toll signaling pathway. *Development* **128,** 4729–4736 (2001).

49. Stokes, B. A., Yadav, S., Shokal, U., Smith, L. & Eleftherianos, I. Bacterial and fungal pattern recognition receptors in homologous innate signaling pathways of insects and mammals. *Frontiers in microbiology* **6,** 19 (2015).

50. Rutschmann, S. *et al.* Role of Drosophila IKK$\gamma$ in a Toll-independent antibacterial immune response. *Nature immunology* **1,** 342 (2000).

51. Rutschmann, S. *et al.* The Rel protein DIF mediates the antifungal but not the antibacterial host defense in Drosophila. *Immunity* **12,** 569–580 (2000).

52. Fernando, M. D. A., Kounatidis, I. & Ligoxygakis, P. Loss of Trabid, a new negative regulator of the Drosophila immune-deficiency pathway at the level of TAK1, reduces life span. *PLoS genetics* **10,** e1004117 (2014).

53. Lhocine, N. *et al.* PIMS modulates immune tolerance by negatively regulating Drosophila innate immune signaling. *Cell host & microbe* **4,** 147–158 (2008).

54. Ryu, J.-H. *et al.* Innate immune homeostasis by the homeobox gene caudal and commensal-gut mutualism in Drosophila. *science* **319,** 777–782 (2008).

55. Ryu, J.-H., Ha, E.-M. & Lee, W.-J. Innate immunity and gut–microbe mutualism in Drosophila. *Developmental & Comparative Immunology* **34,** 369–376 (2010).

56. Dantoft, W. *et al.* The Oct1 homolog Nubbin is a repressor of NF-$\kappa$B-dependent immune gene expression that increases the tolerance to gut microbiota. *BMC biology* **11,** 99 (2013).

57. Whon, T. W. *et al.* Conditionally pathogenic gut microbes promote larval growth by increasing redox-dependent fat storage in high-sugar diet-fed Drosophila. *Antioxidants & redox signaling* **27,** 1361–1380 (2017).

58. Fink, C., Staubach, F., Kuenzel, S., Baines, J. F. & Roeder, T. Non-invasive analysis of microbiome dynamics in the fruit fly Drosophila melanogaster. *Appl. Environ. Microbiol.* **79,** 6984–6988 (2013).

59. Von Frieling, J. *et al.* High fat diet induces a microbiota-dependent increase in stem cell activity in the Drosophila intestine. *bioRxiv,* 604744 (2019).

60. Newell, P. D. & Douglas, A. E. Interspecies interactions determine the impact of the gut microbiota on nutrient allocation in Drosophila melanogaster. *Appl. Environ. Microbiol.* **80,** 788–796 (2014).

61. Huang, J.-H. & Douglas, A. E. Consumption of dietary sugar by gut bacteria determines Drosophila lipid content. *Biology letters* **11,** 20150469 (2015).

62. Yamada, R., Deshpande, S. A., Bruce, K. D., Mak, E. M. & William, W. J. Microbes promote amino acid harvest to rescue undernutrition in Drosophila. *Cell reports* **10,** 865–872 (2015).

63. Leitão-Gonçalves, R. *et al.* Commensal bacteria and essential amino acids control food choice behavior and reproduction. *PLoS Biology* **15,** e2000862 (2017).

64. Shin, S. C. *et al.* Drosophila microbiome modulates host developmental and metabolic homeostasis via insulin signaling. *Science* **334,** 670–674 (2011).

65. Rahim, M. B. H. A. *et al.* Diet-induced metabolic changes of the human gut microbiome: importance of short-chain fatty acids, methylamines and indoles. *Acta diabetologica* **56,** 493–500 (2019).

66. Gao, Z. *et al.* Butyrate improves insulin sensitivity and increases energy expenditure in mice. *Diabetes* **58,** 1509–1517 (2009).

67. Fushimi, T. *et al.* Dietary acetic acid reduces serum cholesterol and triacylglycerols in rats fed a cholesterol-rich diet. *British Journal of Nutrition* **95,** 916–924 (2006).

68. De Vadder, F. *et al.* Microbiota-generated metabolites promote metabolic benefits via gut-brain neural circuits. *Cell* **156,** 84–96 (2014).

69. Yang, Q. & Guan, K.-L. Expanding mTOR signaling. *Cell research* **17,** 666 (2007).

70. Laplante, M. & Sabatini, D. M. mTOR signaling at a glance. *Journal of cell science* **122,** 3589–3594 (2009).

71. Caron, E. *et al.* A comprehensive map of the mTOR signaling network. *Molecular systems biology* **6** (2010).

72. Yang, H. *et al.* mTOR kinase structure, mechanism and regulation. *Nature* **497,** 217 (2013).

73. Schalm, S. S., Fingar, D. C., Sabatini, D. M. & Blenis, J. TOS motif-mediated raptor binding regulates 4E-BP1 multisite phosphorylation and function. *Current biology* **13,** 797–806 (2003).

74. Wang, L., Harris, T. E., Roth, R. A. & Lawrence, J. C. PRAS40 regulates mTORC1 kinase activity by functioning as a direct inhibitor of substrate binding. *Journal of Biological Chemistry* **282,** 20036–20044 (2007).

75. Oh, W. J. & Jacinto, E. mTOR complex 2 signaling and functions. *Cell cycle* **10,** 2305–2316 (2011).

76. Sarbassov, D. D., Guertin, D. A., Ali, S. M. & Sabatini, D. M. Phosphorylation and regulation of Akt/PKB by the rictor-mTOR complex. *Science* **307,** 1098–1101 (2005).

77. Sancak, Y. *et al.* The Rag GTPases bind raptor and mediate amino acid signaling to mTORC1. *Science* **320,** 1496–1501 (2008).

78. Sancak, Y. *et al.* Ragulator-Rag complex targets mTORC1 to the lysosomal surface and is necessary for its activation by amino acids. *Cell* **141,** 290–303 (2010).

79. Saxton, R. A. & Sabatini, D. M. mTOR signaling in growth, metabolism, and disease. *Cell* **168,** 960–976 (2017).

80. Huang, J. & Manning, B. D. The TSC1–TSC2 complex: a molecular switchboard controlling cell growth. *Biochemical Journal* **412,** 179–190 (2008).

81. Wang, X. & Proud, C. G. The mTOR pathway in the control of protein synthesis. *Physiology* **21,** 362–369 (2006).

82. Caron, A., Richard, D. & Laplante, M. The roles of mTOR complexes in lipid metabolism. *Annual review of nutrition* **35,** 321–348 (2015).

83. Düvel, K. *et al.* Activation of a metabolic gene regulatory network downstream of mTOR complex 1. *Molecular cell* **39,** 171–183 (2010).

84. Wang, A., Mouser, J., Pitt, J., Promislow, D. & Kaeberlein, M. Rapamycin enhances survival in a Drosophila model of mitochondrial disease. *Oncotarget* **7,** 80131 (2016).

85. Zhang, H., Stallock, J. P., Ng, J. C., Reinhard, C. & Neufeld, T. P. Regulation of cellular growth by the Drosophila target of rapamycin dTOR. *Genes & development* **14,** 2712–2724 (2000).

86. Goberdhan, D. C., Paricio, N., Goodman, E. C., Mlodzik, M. & Wilson, C. Drosophila tumor suppressor PTEN controls cell size and number by antagonizing the Chico/PI3-kinase signaling pathway. *Genes & development* **13,** 3244–3258 (1999).

87. Kapahi, P. *et al.* Regulation of lifespan in Drosophila by modulation of genes in the TOR signaling pathway. *Current Biology* **14,** 885–890 (2004).

88. Teleman, A. A., Chen, Y.-W. & Cohen, S. M. 4E-BP functions as a metabolic brake used under stress conditions but not during normal growth. *Genes & development* **19,** 1844–1848 (2005).

89. Katewa, S. D. & Kapahi, P. Role of TOR signaling in aging and related biological processes in Drosophila melanogaster. *Experimental gerontology* **46,** 382–390 (2011).

90. Radimerski, T., Montagne, J., Hemmings-Mieszczak, M. & Thomas, G. Lethality of Drosophila lacking TSC tumor suppressor function rescued by reducing dS6K signaling. *Genes & development* **16,** 2627–2632 (2002).

91. Zid, B. M. *et al.* 4E-BP extends lifespan upon dietary restriction by enhancing mitochondrial activity in Drosophila. *Cell* **139,** 149–160 (2009).

92. Seegmiller, A. C. *et al.* The SREBP pathway in Drosophila: regulation by palmitate, not sterols. *Developmental cell* **2,** 229–238 (2002).

93. Kar, S. K. *et al.* Dietary protein sources differentially affect microbiota, mTOR activity and transcription of mTOR signaling pathways in the small intestine. *PloS one* **12,** e0188282 (2017).

94. Kim, K.-A., Gu, W., Lee, I.-A., Joh, E.-H. & Kim, D.-H. High fat diet-induced gut microbiota exacerbates inflammation and obesity in mice via the TLR4 signaling pathway. *PloS one* **7,** e47713 (2012).

95. Storelli, G. *et al.* Lactobacillus plantarum promotes Drosophila systemic growth by modulating hormonal signals through TOR-dependent nutrient sensing. *Cell metabolism* **14,** 403–414 (2011).

96. Pereira, F. C. & Berry, D. Microbial nutrient niches in the gut. *Environmental microbiology* **19,** 1366–1378 (2017).

97. Fan, X. *et al.* Rapamycin preserves gut homeostasis during Drosophila aging. *Oncotarget* **6,** 35274 (2015).

98. Schinaman, J. M., Rana, A., William, W. J., Clark, R. I. & Walker, D. W. Rapamycin modulates tissue aging and lifespan independently of the gut microbiota in Drosophila. *Scientific reports* **9,** 7824 (2019).

99. Bernal, A. & Kimbrell, D. A. Drosophila Thor participates in host immune defense and connects a translational regulator with innate immunity. *Proceedings of the National Academy of Sciences* **97,** 6019–6024 (2000).

100. Charroux, B. *et al.* Cytosolic and secreted peptidoglycan-degrading enzymes in Drosophila respectively control local and systemic immune responses to microbiota. *Cell host & microbe* **23,** 215–228 (2018).

101. Michel, T., Reichhart, J.-M., Hoffmann, J. A. & Royet, J. Drosophila Toll is activated by Gram-positive bacteria through a circulating peptidoglycan recognition protein. *Nature* **414,** 756 (2001).

102. Huang, W. *et al.* Natural variation in genome architecture among 205 Drosophila melanogaster Genetic Reference Panel lines. *Genome research* **24,** 1193–1208 (2014).

103. Gobert, V. *et al.* Dual activation of the Drosophila toll pathway by two pattern recognition receptors. *Science* **302,** 2126–2130 (2003).

104. Chakravorty, S., Helb, D., Burday, M., Connell, N. & Alland, D. A detailed analysis of 16S ribosomal RNA gene segments for the diagnosis of pathogenic bacteria. *Journal of microbiological methods* **69,** 330–339 (2007).

105. Simhadri, R. K. *et al.* The gut commensal microbiome of Drosophila melanogaster is modified by the endosymbiont Wolbachia. *mSphere* **2,** e00287–17 (2017).

106. Merriman, B., R&D Team, I. T. & Rothberg, J. M. Progress in ion torrent semiconductor chip based sequencing. *Electrophoresis* **33,** 3397–3417 (2012).

107. Hammer, Ø., Harper, D. A., Ryan, P. D., *et al.* PAST: paleontological statistics software package for education and data analysis. *Palaeontologia electronica* **4,** 9 (2001).

108. Morris, E. K. *et al.* Choosing and using diversity indices: insights for ecological applications from the German Biodiversity Exploratories. *Ecology and evolution* **4,** 3514–3524 (2014).

109. Gloor, G. B. & Reid, G. Compositional analysis: a valid approach to analyze microbiome high-throughput sequencing data. *Canadian journal of microbiology* **62,** 692–703 (2016).

110. Bland, J. M. & Altman, D. G. The logrank test. *Bmj* **328,** 1073 (2004).

111. Kounatidis, I. *et al.* NF-$\kappa$B immunity in the brain determines fly lifespan in healthy aging and age-related neurodegeneration. *Cell reports* **19,** 836–848 (2017).

112. Livak, K. J. & Schmittgen, T. D. Analysis of relative gene expression data using real-time quantitative PCR and the 2- $\Delta\Delta$CT method. *methods* **25,** 402–408 (2001).

113. Schefe, J. H., Lehmann, K. E., Buschmann, I. R., Unger, T. & Funke-Kaiser, H. Quantitative real-time RT-PCR data analysis: current concepts and the novel "gene expression's C T difference" formula. *Journal of molecular medicine* **84,** 901–910 (2006).

114. Mistry, R., Kounatidis, I. & Ligoxygakis, P. Exploring interactions between pathogens and the Drosophila gut. *Developmental & Comparative Immunology* **64,** 3–10 (2016).

115. Lee, K.-A. *et al.* Bacterial-derived uracil as a modulator of mucosal immunity and gut-microbe homeostasis in Drosophila. *Cell* **153,** 797–811 (2013).

116. Dziarski, R. & Gupta, D. Mammalian peptidoglycan recognition proteins (PGRPs) in innate immunity. *Innate immunity* **16,** 168–174 (2010).

117. Nochi, T. & Kiyono, H. Innate immunity in the mucosal immune system. *Current pharmaceutical design* **12,** 4203–4213 (2006).

118. Moghadam, N. N. *et al.* Strong responses of Drosophila melanogaster microbiota to developmental temperature. *Fly* **12,** 1–12 (2018).

119. Jung, M.-J. *et al.* Chronic repression of mTOR complex 2 induces changes in the gut microbiota of diet-induced obese mice. *Scientific reports* **6,** 30887 (2016).

120. Atilano, M., Glittenberg, M., Bahuguna, S., Wang, L. & Ligoxygakis, P. Drosophila Toll links systemic immunity to long-term intestinal epithelial integrity. *bioRxiv,* 248138 (2018).

121. Kleino, A. *et al.* Pirk is a negative regulator of the Drosophila Imd pathway. *The Journal of Immunology* **180,** 5413–5422 (2008).

122. Aggarwal, K. *et al.* Rudra interrupts receptor signaling complexes to negatively regulate the IMD pathway. *PLoS pathogens* **4,** e1000120 (2008).

123. Bischoff, V. *et al.* Downregulation of the Drosophila immune response by peptidoglycan-recognition proteins SC1 and SC2. *PLoS pathogens* **2,** e14 (2006).

124. Vaz, F. *et al.* Accessibility to Peptidoglycan Is Important for the Recognition of Gram-Positive Bacteria in Drosophila. *Cell reports* **27,** 2480–2492 (2019).

125. Kuraishi, T., Kanoh, H., Momiuchi, Y., Kenmoku, H. & Kurata, S. in *Chronic Inflammation* 119–129 (Springer, 2016).

126. Shroff, K. E., Meslin, K. & Cebra, J. J. Commensal enteric bacteria engender a self-limiting humoral mucosal immune response while permanently colonizing the gut. *Infection and immunity* **63,** 3904–3913 (1995).

127. Mantis, N. J., Rol, N. & Corthésy, B. Secretory IgA's complex roles in immunity and mucosal homeostasis in the gut. *Mucosal immunology* **4,** 603 (2011).

128. Bunker, J. J. & Bendelac, A. IgA responses to microbiota. *Immunity* **49,** 211–224 (2018).

129. Werner, T. *et al.* A family of peptidoglycan recognition proteins in the fruit fly Drosophila melanogaster. *Proceedings of the National Academy of Sciences* **97,** 13772–13777 (2000).

130. De Gregorio, E., Spellman, P. T., Rubin, G. M. & Lemaitre, B. Genome-wide analysis of the Drosophila immune response by using oligonucleotide microarrays. *Proceedings of the National Academy of Sciences* **98,** 12590–12595 (2001).

131. De Gregorio, E., Spellman, P. T., Tzou, P., Rubin, G. M. & Lemaitre, B. The Toll and Imd pathways are the major regulators of the immune response in Drosophila. *The EMBO journal* **21,** 2568–2579 (2002).

132. Kimball, S. R. *et al.* Interaction between the AMP-activated protein kinase and mTOR signaling pathways. *Medicine and science in sports and exercise* **38,** 1958 (2006).

133. Bitto, A. *et al.* Transient rapamycin treatment can increase lifespan and healthspan in middle-aged mice. *elife* **5,** e16351 (2016).

134. Zhang, Y. *et al.* Lactobacillus casei protects dextran sodium sulfate- or rapamycin-induced colonic inflammation in the mouse. *European journal of nutrition,* 1–9 (2019).

135. Kang, M.-J. *et al.* 4E-BP is a target of the GCN2–ATF4 pathway during Drosophila development and aging. *J Cell Biol* **216,** 115–129 (2017).